International Journal of Computer Vision, 10:1, 67–84 (1993)

Interpretation of Conic Motion and Its Applications

WU LIU AND KENICHI KANATANI
Department of Computer Science, Gunma University, Kiryu, Gunma 376, Japan

Received January, 1992. Revised November, 1992.

Abstract
The indeterminacy of conic motion is analyzed in terms of Lie group theory. It is shown that an image motion of a conic is associated with a group of *invisible motions* that do not cause a visible change of the conic. All such groups are isomorphic to the group associated with a special conic called the *standard circle*, for which the group of invisible motions is the (three-dimensional) *Lorentz group*. Similar results are obtained for *invisible optical flows*. Finally, our analysis is extended to *conic stereo*: the 3-D position and orientation of a conic in the scene are computed from two projections. This algorithm also works with one camera if a circular pattern is projected from a light source.

1 Introduction

"Conics" provide the most important clues to 3-D interpretation of images next to straight lines. This is because many man-made objects have circular parts, and circles are perspectively projected onto conics. For example, if a robot is to operate in an industrial environment (say, in a nuclear power station), it must recognize circular gauges, meters, dials, handles, and other circular objects by finding conics on the image plane. Detected conics not only provide clues to object recognition; if their true shapes are known, their 3-D geometry is also computed analytically [6, 13, 15, 21, 23, 24].

In this article, we study *how much information is available if a motion of a single conic is observed on the image plane.* This problem originates from "contour-based optical flow determination" [4, 8, 9, 10, 30, 31, 32]. For this, conics appear to be the best candidate. However, Bergholm [1] pointed out that many types of familiar curves, including conics, are incapable of determining optical flow; such "ambiguous curves" were classified in detail by Bergholm and Carlsson [2].

Here, we concentrate on conics and analyze the indeterminacy by invoking Lie group theory [10]. We first describe the representation of conics in terms of *N-vectors* and discuss fundamental properties of conics. We then show that an image motion of a conic is associated with a group of *invisible motions* that do not cause a visible change of the conic. All such groups are isomorphic to the group associated with a special conic called *standard circle*, for which the group of invisible motions is the (three-dimensional) *Lorentz group*. Similar results are obtained for *invisible optical flows*.

Finally, our theoretical analysis is extended to a practical method for eliminating the ambiguity. We call it *conic stereo*: the 3-D position and orientation of a conic in the scene are computed from two projections obtained by two fixed cameras. This algorithm also works with one camera if a circular pattern is projected from a light source. Some real image examples are given.

2 N-Vectors and Collineations

Assume the following camera imaging model. The camera is associated with an XYZ coordinate system with origin O at the center of the lens and Z axis along the optical axis (figure 1). The plane $Z = f$ is identified with the image plane, on which an xy image coordinate system is defined so that the x and y axes are parallel to the X and Y axes, respectively. Let us call the origin O the *viewpoint* and the constant f the *focal length.*

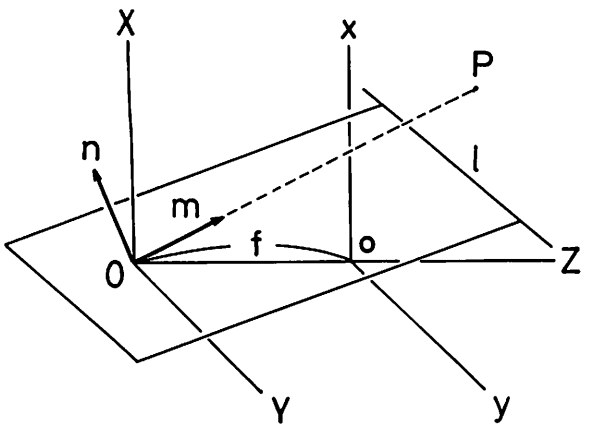

Fig. 1. Camera imaging geometry and N-vectors of a point and a line.

A point (x, y) on the image plane is represented by the unit vector $\mathbf{m}$ indicating the orientation of the ray starting from the viewpoint O and passing through that point; a line $Ax + By + C = 0$ on the image plane is represented by the unit surface normal $\mathbf{n}$ to the plane passing through the viewpoint O and intersecting the image plane along that line (figure 1). Their components are given by

$$\mathbf{m} = \pm N\left[\begin{pmatrix} x \\ y \\ f \end{pmatrix}\right] \qquad \mathbf{n} = \pm N\left[\begin{pmatrix} A \\ B \\ C/f \end{pmatrix}\right] \quad (1)$$

where $N[\cdot]$ denotes normalization into a unit vector. We call $\mathbf{m}$ and $\mathbf{n}$ the *N-vectors* of the point and the line [11]. If $\mathbf{m}$ and $\mathbf{n}$ are the N-vectors of a point P and a line l, respectively, it is immediately seen that point P is *on* line l, or line l *passes through* point P, if and only if

$$(\mathbf{m}, \mathbf{n}) = 0 \quad (2)$$

where $(\cdot, \cdot)$ denotes the inner product of vectors. If this equation is satisfied, we also say that point P and line l are *incident* to each other. We call equation (2) the *incidence equation*.

The use of N-vectors for representing points and lines on the image plane is equivalent to using *homogeneous coordinates* [26]. Although homogeneous coordinates can be multiplied by any nonzero number, computational problems arise if they are too large or too small. So, it is convenient to normalize them into a unit vector, which is precisely the N-vector as defined above. Rewriting the relationships of projective geometry as *computational procedures* in terms of N-vectors, Kanatani [11] called the resulting formulation *computational projective geometry*. Here, we adopt this formulation, regarding a unit vector $\mathbf{m}$ whose Z-component is 0 as the N-vector of an *ideal point* (a *point at infinity*) and $\mathbf{n} = (0, 0, \pm 1)$ as the N-vector of the *ideal line* (the *line at infinity*).

Points are *collinear* if they are all on a common line; lines are *concurrent* if they all meet at a common point. A *collineation* [26] is a one-to-one mapping between points (including ideal points) and between lines (including the ideal line) such that (i) collinear points are mapped to collinear points, (ii) concurrent lines are mapped to concurrent lines, and (iii) incidence is preserved—if a point (or line) is on (or passes through) a line (or point), the mapped point (or line) is on (or passes through) the mapped line (or point). It can be proved that a collineation maps a point of N-vector $\mathbf{m}$ to a point of N-vector $\mathbf{m}'$, and a line of N-vector $\mathbf{n}$ to a line of N-vector $\mathbf{n}'$, in the form

$$\mathbf{m}' = \pm N[\mathbf{A}^{\mathrm{T}}\mathbf{m}] \qquad \mathbf{n}' = +N[\mathbf{A}^{-1}\mathbf{n}] \quad (3)$$

where $\mathbf{A}$ is a nonsingular matrix and T denotes transpose (see [13] for details). In order to eliminate the scale indeterminacy, we hereafter adopt the convention that $\mathbf{A}$ is scaled so that $\det \mathbf{A} = 1$. For simplicity, let us call the collineation represented by matrix $\mathbf{A}$ simply "collineation $\mathbf{A}$." In *inhomogeneous coordinates* (i.e., image coordinates), the first of equations (3) for $\mathbf{A} = (A_{ij})$ $i, j = 1, 2, 3$, is rewritten as

$$x' = f\frac{A_{11}x + A_{21}y + A_{31}f}{A_{13}x + A_{23}y + A_{33}f}$$

$$y' = f\frac{A_{12}x + A_{22}y + A_{32}f}{A_{13}x + A_{23}y + A_{33}f} \quad (4)$$

The set of all collineations is the *group of 2-D projective transformations* [26], which is isomorphic to $SL(3)$—the group of three-dimensional matrices of determinant 1 under matrix multiplication: the composition of collineation $\mathbf{A}_1$ followed by collineation $\mathbf{A}_2$ coincides with collineation $\mathbf{A}_1\mathbf{A}_2$, and the inverse of collineation $\mathbf{A}$ is given by collineation $\mathbf{A}^{-1}$. A collineation is also called a *projective transformation* or simply *projectivity* [26].

3 Fundamental Properties of Conics

A quadratic curve on the image plane has the form

$$Ax^2 + 2Bxy + Cy^2 + 2(Dx + Ey) + F = 0 \quad (5)$$

In terms of N-vector $\mathbf{m}$, this equation is written as

$$(\mathbf{m}, \mathbf{Qm}) = 0 \qquad \mathbf{Q} = \kappa \begin{pmatrix} A & B & D/f \\ B & C & E/f \\ D/f & E/f & F/f^2 \end{pmatrix} \tag{6}$$

where κ is an arbitrary nonzero constant. For brevity, we hereafter refer to the conic represented by matrix $\mathbf{Q}$ as simply "conic $\mathbf{Q}$." In order to eliminate the scale indeterminacy, we choose the constant κ so that $\det \mathbf{Q} = -1$ (this choice is natural for real conics) whenever $\det \mathbf{Q} \neq 0$.

Conics are always projected onto conics not only by perspective projections but also by general collineations. It is easy to show that the transformation rule of conics under a collineation is as follows.

Proposition 1. Collineation $\mathbf{A}$ maps conic $\mathbf{Q}$ to conic $\mathbf{Q}'$ in the form

$$\mathbf{Q}' = \mathbf{A}^{-1}\,\mathbf{Q}(\mathbf{A}^{-1})^{\mathsf{T}} \tag{7}$$

Let us say that a collineation that maps a conic $\mathbf{Q}$ to itself *preserves* the conic $\mathbf{Q}$. The following are immediate consequences of proposition 1.

Proposition 2. A collineation $\mathbf{A}$ preserves a conic $\mathbf{Q}$ if and only if

$$\mathbf{AQA}^{\mathsf{T}} = \mathbf{Q} \tag{8}$$

Proposition 3. The set of all collineations that preserve a conic is a subgroup of the group of 2-D projective transformations.

A conic is *proper* if it does not consist of two (real or imaginary) lines or one degenerate (real or imaginary) line, or equivalently if equation (5) is irreducible in the complex domain. The following facts are well known:

Proposition 4. A conic $\mathbf{Q}$ is proper if and only if the corresponding $\mathbf{Q}$ is nonsingular.

Proposition 5. A proper conic $\mathbf{Q}$ is a real conic if and only if the signature of the matrix $\mathbf{Q}$ is (2, 1).

Here, the *signature* of a symmetric matrix is the pair (p, q), where p is the number of its positive eigenvalues and q is the number of its negative eigenvalues. In the following, we only consider proper real conics (with signature (2, 1) and determinant -1).

4 Group of Invisible Motions

Given two conics $\mathbf{Q}$ and $\mathbf{Q}'$ on the image plane, the collineation $\mathbf{A}$ that maps conic $\mathbf{Q}$ to conic $\mathbf{Q}'$ is not uniquely determined: if $\mathbf{L}$ and $\mathbf{L}'$ are collineations that preserve $\mathbf{Q}$ and $\mathbf{Q}'$ respectively, the composition of $\mathbf{L}$, $\mathbf{A}$, and $\mathbf{L}'$ in this order is also a collineation that maps conic $\mathbf{Q}$ to conic $\mathbf{Q}'$. Let us call a collineation $\mathbf{L}$ an *invisible* (*image*) *motion* of conic $\mathbf{Q}$ if $\mathbf{L}$ preserves $\mathbf{Q}$. From proposition 2, the set $\mathcal{H}_{\mathbf{Q}}$ of all collineations that preserve conic $\mathbf{Q}$ is given by

$$\mathcal{H}_{\mathbf{Q}} = \{\mathbf{L} |\ \det \mathbf{L} = 1,\ \mathbf{LQL}^{\mathsf{T}} = \mathbf{Q}\} \tag{9}$$

This is a group of transformations (proposition 3). We call it the *group of invisible motions* of $\mathbf{Q}$. The equation $\mathbf{LQL}^{\mathsf{T}} = \mathbf{Q}$ is a constraint on a symmetric matrix of determinant -1, providing five independent equations. Since a general collineation (i.e., a nonsingular matrix of determinant 1) has eight independent parameters, the group $\mathcal{H}_{\mathbf{Q}}$ has three degrees of freedom. Hence, the group of invisible motions is a *three-dimensional Lie group* [10]. It is easy to prove the following proposition.

Proposition 6. Let $\mathbf{A}_0$ be a particular collineation that maps conic $\mathbf{Q}$ to conic $\mathbf{Q}'$. For any collineation $\mathbf{A}$ that maps conic $\mathbf{Q}$ to conic $\mathbf{Q}'$, there exist $\mathbf{L} \in \mathcal{H}_{\mathbf{Q}}$ and $\mathbf{L}' \in \mathcal{H}_{\mathbf{Q}'}$ such that

$$\mathbf{A} = \mathbf{LA}_0 = \mathbf{A}_0\mathbf{L}' \tag{10}$$

and they are uniquely determined by $\mathbf{A}_0$.

Corollary 1: *All collineations that map conic* $\mathbf{Q}$ *to conic* $\mathbf{Q}'$ *are exhausted by a particular collineation* $\mathbf{A}_0$ *and either* $\mathcal{H}_{\mathbf{Q}}$ *or* $\mathcal{H}_{\mathbf{Q}'}$.

The above statement is summarized by saying that if $\mathbf{A}_0$ is a particular collineation that maps conic $\mathbf{Q}$ to conic $\mathbf{Q}'$, the set of all such collineations is given by

$$\mathcal{H}_{\mathbf{Q}}\mathbf{A}_0 = \mathbf{A}_0\mathcal{H}_{\mathbf{Q}'} = \mathcal{H}_{\mathbf{Q}}\mathbf{A}_0\mathcal{H}_{\mathbf{Q}'} \tag{11}$$

The set $\mathcal{H}_{\mathbf{Q}}\mathbf{A}_0$ is called the *right coset* of $\mathbf{A}_0$ by $\mathcal{H}_{\mathbf{Q}}$, and the set $\mathbf{A}_0\mathcal{H}_{\mathbf{Q}'}$ is called the *left coset* of $\mathbf{A}_0$ by $\mathcal{H}_{\mathbf{Q}'}$. The set $\mathcal{H}_{\mathbf{Q}}\mathbf{A}_0\mathcal{H}_{\mathbf{Q}'}$ is called to be the *double coset* of $\mathbf{A}_0$ by $\mathcal{H}_{\mathbf{Q}}$ and $\mathcal{H}_{\mathbf{Q}'}$. Define a mapping $t_{\mathbf{A}_0} : \mathcal{H}_{\mathbf{Q}} \to \mathcal{H}_{\mathbf{Q}'}$ by

$$t_{\mathbf{A}_0}(\mathbf{L}) = \mathbf{A}_0^{-1}\mathbf{LA}_0 \tag{12}$$

It is easy to confirm that $t_{\mathbf{A}_0}(\mathbf{L}_1\mathbf{L}_2) = t_{\mathbf{A}_0}(\mathbf{L}_1)t_{\mathbf{A}_0}(\mathbf{L}_2)$ for $\mathbf{L}_1, \mathbf{L}_2 \in \mathcal{H}_{\mathbf{Q}}$. Hence, $t_{\mathbf{A}_0}$ is a *homomorphism* from $\mathcal{H}_{\mathbf{Q}}$ to $\mathcal{H}_{\mathbf{Q}'}$. It is also easy to see that $t_{\mathbf{A}_0}$ is a *one-to-one* and *onto* mapping. This means that

$$\mathcal{H}_{\mathbf{Q}'} = \mathbf{A}_0^{-1}\,\mathcal{H}_{\mathbf{Q}}\mathbf{A}_0 \tag{13}$$

If there exists a collineation $\mathbf{A}_0$ such that this equation holds for two groups $\mathcal{H}_{\mathbf{Q}}$ and $\mathcal{H}_{\mathbf{Q}'}$, group $\mathcal{H}_{\mathbf{Q}}$ is said

to be *conjugate* to $\mathcal{H}_{\mathbf{Q}'}$. If two groups are conjugate to each other, they are isomorphic to each other: $\mathcal{H}_{\mathbf{Q}} \cong \mathcal{H}_{\mathbf{Q}'}$.

5 Mapping of Conics

Given two conics $\mathbf{Q}$ and $\mathbf{Q}'$, a particular collineation that maps conic $\mathbf{Q}$ to conic $\mathbf{Q}'$ is easily constructed. Form proposition 1, what we want is a nonsingular matrix $\mathbf{A}_0$ such that

$$\mathbf{A}_0\mathbf{A}'\mathbf{A}_0^{\mathsf{T}} = \mathbf{Q} \tag{14}$$

Since $\mathbf{Q}$ and $\mathbf{Q}'$ are both symmetric matrices with signature (2, 1), we can find orthogonal matrices $\mathbf{U}$ and $\mathbf{U}'$ that diagonalize them in the form

$$\begin{aligned} \mathbf{U}^{\mathsf{T}}\mathbf{Q}\mathbf{U} &= \operatorname{diag}(\lambda_1, \lambda_2, \lambda_3) \\ \mathbf{U}^{\mathsf{T}}\mathbf{Q}'\mathbf{U}' &= \operatorname{diag}(\lambda_1', \lambda_2', \lambda_3') \end{aligned} \tag{15}$$

for $\lambda_1, \lambda_2 > 0$, $\lambda_3 < 0$ and $\lambda_1', \lambda_2' > 0$, $\lambda_3' < 0$, where diag $(\cdot, \cdot, \cdot)$ denotes the diagonal matrix with the indicated diagonal elements in that order. Since the two conics both have signature (2, 1), the orthogonal matrices $\mathbf{U}$ and $\mathbf{U}'$ can be chosen so that corresponding eigenvalues of $\mathbf{Q}$ and $\mathbf{Q}'$ have the same signs. Let

$$\mathbf{A}_0 = \mathbf{U} \operatorname{diag}\left(\sqrt{\lambda_1/\lambda_1'}, \sqrt{\lambda_2/\lambda_2'}, \sqrt{\lambda_3/\lambda_3'}\right)\mathbf{U}'^{\mathsf{T}} \tag{16}$$

It is easy to confirm that $\det \mathbf{A}_0 = 1$ and equation (14) is satisfied. Thus, we have the following.

Proposition 7. For any two real proper conics, there exists a collineation that maps one to the other.

Example. Consider a particular collineation that maps ellipse

$$\frac{x^2}{a^2} + \frac{y^2}{b^2} = 1 \qquad a, b > 0 \tag{17}$$

to hyperbola

$$\frac{x^2}{\alpha^2} - \frac{y^2}{\beta^2} = 1 \qquad \alpha, \beta > 0 \tag{18}$$

Their respective matrix representations are

$$\begin{aligned} \mathbf{Q} &= \kappa \operatorname{diag}\left(\frac{1}{a^2}, \frac{1}{b^2}, -\frac{1}{f^2}\right) \\ \mathbf{Q}' &= \kappa' \operatorname{diag}\left(\frac{1}{\alpha^2}, \frac{1}{\beta^2}, \frac{1}{f^2}\right) \end{aligned} \tag{19}$$

where $\kappa = (abf)^{2/3}$ and $\kappa' = (\alpha\beta f)^{2/3}$. Matrix $\mathbf{Q}$ is in canonical form as is. Matrix $\mathbf{Q}'$ is transformed into canonical form as follows:

$$\begin{aligned} &\kappa' \begin{pmatrix} 0 & 1 & 0 \\ 0 & 0 & 1 \\ 1 & 0 & 0 \end{pmatrix} \begin{pmatrix} -1/\alpha^2 & 0 & 0 \\ 0 & 1/\beta^2 & 0 \\ 0 & 0 & 1/f^2 \end{pmatrix} \begin{pmatrix} 0 & 0 & 1 \\ 1 & 0 & 0 \\ 0 & 1 & 0 \end{pmatrix} \\ &= \kappa' \operatorname{diag}\left(\frac{1}{\beta^2}, \frac{1}{f^2}, -\frac{1}{\alpha^2}\right) \end{aligned} \tag{20}$$

Hence, a particular collineation $\mathbf{A}_0$ that maps conic $\mathbf{Q}$ to conic $\mathbf{Q}'$ is given by

$$\begin{aligned} \mathbf{A}_0 &= \sqrt{\frac{\kappa}{\kappa'}} \begin{pmatrix} 1 & 0 & 0 \\ 0 & 1 & 0 \\ 0 & 0 & 1 \end{pmatrix} \begin{pmatrix} \beta/a & 0 & 0 \\ 0 & f/b & 0 \\ 0 & 0 & \alpha/f \end{pmatrix} \begin{pmatrix} 0 & 1 & 0 \\ 0 & 0 & 1 \\ 1 & 0 & 0 \end{pmatrix} \\ &= \sqrt{\frac{\kappa}{\kappa'}} \begin{pmatrix} 0 & \beta/a & 0 \\ 0 & 0 & f/b \\ \alpha/f & 0 & 0 \end{pmatrix} \end{aligned} \tag{21}$$

In image coordinates (see equations (4)),

$$x' = \frac{b\alpha}{y} \qquad y' = \frac{b\beta x}{ay} \tag{22}$$

6 Standard Circle

Let $\mathbf{J}$ be a circle of radius f centered at the image origin:

$$x^2 + y^2 = f^2 \tag{23}$$

In matrix form,

$$\mathbf{J} = \operatorname{diag}(1, 1, -1) \tag{24}$$

Let us call $\mathbf{J}$ the *standard circle*. Proposition 7 implies that for any conic $\mathbf{Q}$ there exists a collineation that maps it to the standard circle $\mathbf{J}$. Let us call such a collineation a *standardizing collineation*. The group $\mathcal{H}_{\mathbf{J}}$ of invisible motions of the standard circle $\mathbf{J}$ is

$$\mathcal{H}_{\mathbf{J}} = \{\mathbf{L} \mid \det \mathbf{L} = 1, \mathbf{L}\mathbf{J}\mathbf{L}^{\mathsf{T}} = \mathbf{J}\} \tag{25}$$

This group is known as the three-dimensional (or "2+1-dimensional") proper *Lorentz group*. Then, as shown in section 4, the group $\mathcal{H}_{\mathbf{Q}}$ of invisible motions of any conic $\mathbf{Q}$ is given by

$$\mathcal{H}_{\mathbf{Q}} = \mathbf{A}_{\mathbf{Q}}\mathcal{H}_{\mathbf{J}}\mathbf{A}_{\mathbf{Q}}^{-1} \tag{26}$$

where $\mathbf{A}_{\mathbf{Q}}$ is an arbitrary standardizing collineation of conic $\mathbf{Q}$. Hence, *the group $\mathcal{H}_{\mathbf{Q}}$ of invisible motions of any conic $\mathbf{Q}$ is isomorphic to the Lorentz group $\mathcal{H}_{\mathbf{J}}$.*

It follows that the set of all collineations that map $\mathbf{Q}$ to $\mathbf{Q}'$ is given by

$$\mathbf{A}_{\mathbf{Q}'}\mathcal{H}_J\mathbf{A}_{\mathbf{Q}}^{-1} \tag{27}$$

where $\mathbf{A}_{\mathbf{Q}}$ and $\mathbf{A}_{\mathbf{Q}'}$ are arbitrary standardizing collineations of conic $\mathbf{Q}$ and $\mathbf{Q}'$, repectively.

The Lorentz group $\mathcal{H}_J$ has many subgroups. The following three are one-parameter subgroups that generate $\mathcal{H}_J$:

$$\mathbf{L}_1(t) = \begin{bmatrix} \cosh t & 0 & \sinh t \\ 0 & 1 & 0 \\ \sinh t & 0 & \cosh t \end{bmatrix}$$

$$\mathbf{L}_2(t) = \begin{bmatrix} 1 & 0 & 0 \\ 0 & \cosh t & \sinh t \\ 0 & \sinh t & \cosh t \end{bmatrix}$$

$$\mathbf{L}_3(t) = \begin{bmatrix} \cos t & \sin t & 0 \\ -\sin t & \cos t & 0 \\ 0 & 0 & 1 \end{bmatrix} \tag{28}$$

In image coordinates (see equations (4)),

$$\mathbf{L}_1(t) : x' = f\frac{x\cosh t + f\sinh t}{x\sinh t + f\cosh t}$$

$$y' = \frac{fy}{x\sinh t + f\cosh t} \tag{29}$$

$$\mathbf{L}_2(t) : x' = \frac{fx}{y\sinh t + f\cosh t}$$

$$y' = \mathrm{f}\frac{y\cosh t + f\sinh t}{y\sinh t + f\cosh t} \tag{30}$$

$$\mathbf{L}_3(t) : x' = x\cos t - y\sin t$$

$$y' = x\sin t + y\cos t \tag{31}$$

The collineation $\mathbf{L}_3(t)$ rotates the image plane around its origin by angle t. The standard circle J is evidently kept invariant. It is easy to confirm that $\mathbf{L}_1(t)$ and $\mathbf{L}_2(t)$ also map the standard circle $\mathbf{J}$ to itself.

7 Representation of Invisible Flows

We now consider infinitesimal image motion. It can be shown [11, 13] that the optical flow induced by an infinitesimal collineation has the form

$$\dot{\mathbf{m}} = \mathbf{W}^{\mathrm{T}}\mathbf{m} - (\mathbf{m}, \mathbf{W}^{\mathrm{T}}\mathbf{m})\mathbf{m} \tag{32}$$

where $\mathbf{W}$ is a matrix of trace 0. Let us call the time derivative $\dot{\mathbf{m}}$ of N-vector $\mathbf{m}$ the *N-velocity*, and matrix $\mathbf{W}$ the *flow matrix*. For simplicity, we identify an optical flow with its flow matrix $\mathbf{W}$ and call it simply "optical flow $\mathbf{W}$." There is no ambiguity in talking about addition of two flows, since componentwise addition of N-velocities or image velocities is equivalent to addition of the corresponding flow matrices.

We call an optical flow that does not cause any visible change of conic $\mathbf{Q}$ an *invisible flow* of conic $\mathbf{Q}$. Let $\mathbf{L} = \mathbf{I} + \mathbf{W}\,\Delta t + O(\Delta t^2)$ be a small invisible collineation of conic $\mathbf{Q}$. Substituting this into the invisibility condition $\mathbf{LQL}^{\mathrm{T}} = \mathbf{Q}$ (equation (9)) and taking the limit as $\Delta t \to 0$, we obtain the next proposition.

Proposition 8. An optical flow $\mathbf{W}$ is an invisible flow of conic $\mathbf{Q}$ if and only if

$$\mathbf{WQ} + \mathbf{QW}^{\mathrm{T}} = \mathbf{O} \tag{33}$$

The set

$$h_{\mathbf{Q}} = \{\mathbf{W} | \mathbf{WQ} + \mathbf{QW}^{\mathrm{T}} = \mathbf{O}\} \tag{34}$$

of all invisible flows of conic $\mathbf{Q}$ is the *Lie algebra* of the group $\mathcal{H}_{\mathbf{Q}}$ of invisible motions of conic $\mathbf{Q}$. Since $\mathcal{H}_{\mathbf{Q}}$ is a three-dimensional Lie group, its Lie algebra $h_{\mathbf{Q}}$ is a *three-dimensional linear space* with respect to matrix addition and scalar multiplication. Its basis is easily constructed as follows:

Proposition 9. Any invisible flow $\mathbf{W}$ of conic $\mathbf{Q}$ is uniquely expressed in the form

$$\mathbf{W} = c_1\mathbf{K}_1 + c_2\mathbf{K}_2 + c_3\mathbf{K}_3 \tag{35}$$

for some c_1, c_2, and c_3, where

$$\mathbf{K}_1 = \begin{bmatrix} -Q_{31}^{-1} & -Q_{32}^{-1} & -Q_{33}^{-1} \\ 0 & 0 & 0 \\ Q_{11}^{-1} & Q_{12}^{-1} & Q_{13}^{-1} \end{bmatrix}$$

$$\mathbf{K}_2 = \begin{bmatrix} 0 & 0 & 0 \\ -Q_{31}^{-1} & -Q_{32}^{-1} & -Q_{33}^{-1} \\ Q_{21}^{-1} & Q_{22}^{-1} & Q_{23}^{-1} \end{bmatrix}$$

$$\mathbf{K}_3 = \begin{bmatrix} Q_{21}^{-1} & Q_{22}^{-1} & Q_{23}^{-1} \\ -Q_{11}^{-1} & -Q_{12}^{-1} & -Q_{13}^{-1} \\ 0 & 0 & 0 \end{bmatrix} \tag{36}$$

and Q_{ij}^{-1} is the (i, j) element of the inverse $\mathbf{Q}^{-1}$.

Proof: Since $\mathbf{Q}$ is a symmetric matrix, the condition $\mathbf{WQ} + \mathbf{QW}^{\mathrm{T}} = \mathbf{O}$ is rewritten as $(\mathbf{WQ})^{\mathrm{T}} = -\mathbf{WQ}$. This means that matrix $\mathbf{WQ}$ is an antisymmetric matrix. Hence, we can write

$$\mathbf{WQ} = \begin{pmatrix} 0 & c_3 & -c_1 \\ -c_3 & 0 & -c_2 \\ c_1 & c_2 & 0 \end{pmatrix} \tag{37}$$

for some c_1, c_2, and c_3. Thus,

$$\mathbf{W} = \left[c_1 \begin{pmatrix} 0 & 0 & -1 \\ 0 & 0 & 0 \\ 1 & 0 & 0 \end{pmatrix} + c_2 \begin{pmatrix} 0 & 0 & 0 \\ 0 & 0 & -1 \\ 0 & 1 & 0 \end{pmatrix} + c_3 \begin{pmatrix} 0 & 1 & 0 \\ -1 & 0 & 0 \\ 0 & 0 & 0 \end{pmatrix} \right] \mathbf{Q}^{-1} \tag{38}$$

from which follow equations (35) and (36). Evidently, matrixes $\mathbf{K}_1$, $\mathbf{K}_2$, and $\mathbf{K}_3$ are linearly independent. Hence, the expression of equation (35) is unique. ■

Example. Consider an ellipse in the form of

$$\frac{x^2}{a^2} + \frac{y^2}{b^2} = 1 \qquad a > 0, \quad b > 0 \tag{39}$$

In matrix form,

$$\mathbf{Q} = \kappa \operatorname{diag}\left(\frac{1}{a^2}, \frac{1}{b^2}, -\frac{1}{f^2} \right)$$

$$\mathbf{Q}^{-1} = \frac{1}{\kappa} \operatorname{diag}(a^2, b^2, -f^2) \tag{40}$$

where $\kappa = (abf)^{2/3}$. If we define $\{\mathbf{K}_1, \mathbf{K}_2, \mathbf{K}_3\}$ by equations (36) multiplied by κ/f^2, the general form of invisible flow is given by

$$\mathbf{W} = c_1 \begin{pmatrix} 0 & 0 & 0 \\ 0 & 0 & 0 \\ a^2/f^2 & 0 & 0 \end{pmatrix} + c_2 \begin{pmatrix} 0 & 0 & 0 \\ 0 & 0 & 1 \\ 0 & b^2/f^2 & 0 \end{pmatrix} + c_3 \begin{pmatrix} 0 & b^2/f^2 & 0 \\ -a^2/f^2 & 0 & 0 \\ 0 & 0 & 0 \end{pmatrix} \tag{41}$$

This flow is a superposition of the following three flows:

$$\dot{x} = -\frac{1}{f}(x^2 - a^2), \qquad \dot{y} = -\frac{1}{f} xy \tag{42}$$

$$\dot{x} = -\frac{1}{f} xy, \qquad \dot{y} = -\frac{1}{f}(y^2 - b^2) \tag{43}$$

$$\dot{x} = -\frac{a^2}{f^2} y, \qquad \dot{y} = \frac{b^2}{f^2} x \tag{44}$$

These flows are shown in figures 2(a), (b), and (c), respectively.

The isomorphism between groups of invisible motions can also be applied to the spaces of invisible flows. It is easy to prove the next proposition.

Proposition 10. The mapping $t_{\mathbf{A}_0} : h_{\mathbf{Q}} \to h_{\mathbf{Q}'}$ defined by

$$t_{\mathbf{A}_0}(\mathbf{W}) = \mathbf{A}_0^{-1} \mathbf{W} \mathbf{A}_0 \tag{45}$$

for a particular collineation $\mathbf{A}_0$ that maps conic $\mathbf{Q}$ to conic $\mathbf{Q}'$ is a nonsingular linear mapping from $h_{\mathbf{Q}}$ onto $h_{\mathbf{Q}'}$.

The mapping $t_{\mathbf{A}_0}$ is called the *adjoint transformation* of the corresponding Lie group isomorphism [10]. This adjoint transformation can also be defined when $\mathbf{Q} = \mathbf{Q}'$. Namely,

Corollary 2: The mapping $t_{\mathbf{L}_0} : h_{\mathbf{Q}} \to h_{\mathbf{Q}}$ defined by

$$t_{\mathbf{L}_0}(\mathbf{W}) = \mathbf{L}_0^{-1} \mathbf{W} \mathbf{L}_0 \tag{46}$$

for an invisible motion $\mathbf{L}_0$ of conic $\mathbf{Q}$ is a nonsingular linear mapping from $h_{\mathbf{Q}}$ to itself.

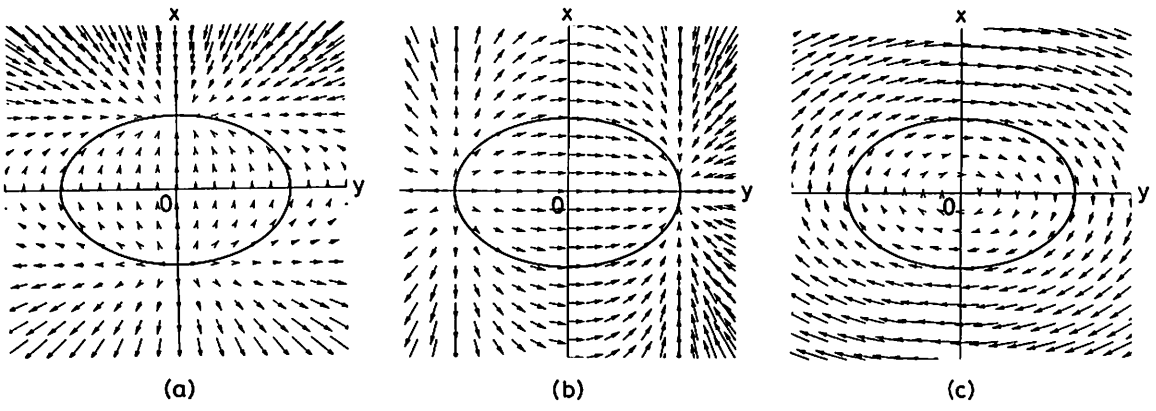

Fig. 2. Invisible flows of an ellipse centered at the image origin.

8 Deformation of a Conic

Consider a smoothly deforming conic $\mathbf{Q}(t)$, assuming that it is always kept to be a real proper conic while deforming. Define its *deformation* $\mathbf{D}$ at time t by

$$\mathbf{D} = \dot{\mathbf{Q}}(t)\mathbf{Q}(t)^{-1} = \lim_{\Delta t \to 0} \frac{\mathbf{Q}(t + \Delta t) - \mathbf{Q}(t)}{\Delta t} \mathbf{Q}(t)^{-1} \tag{47}$$

The deformation $\mathbf{D}$ cannot be an arbitrary matrix. Firstly, $\mathbf{Q}(t)$ must always be kept symmetric. This requirement is written as $\mathbf{DQ}(t)\ \mathbf{Q}(t)\mathbf{D}^{\mathsf{T}}$. Secondly, $\mathbf{Q}$ is always scaled so that $\det \mathbf{Q} = -1$, so the constraint $\operatorname{tr} \mathbf{D} = 0$ must be assigned.

Define the following set:

$$\mathfrak{D}_{\mathbf{Q}} = \{\mathbf{D} | \operatorname{tr} \mathbf{D} = 0,\ \mathbf{DQ} = \mathbf{QD}^{\mathsf{T}}\} \tag{48}$$

(The condition that the signature should not change need not be considered—the signature is a pair of "integers," so it is not affected by a "continuous" motion.) The set $\mathfrak{D}_{\mathbf{Q}}$ is a linear space: if $\mathbf{D}_1, \mathbf{D}_2 \in \mathfrak{D}_{\mathbf{Q}}$, then $c_1\mathbf{D}_1 + c_2\mathbf{D}_2 \in \mathfrak{D}_{\mathbf{Q}}$ for any c_1 and c_2. The condition $\mathbf{DQ} = \mathbf{QD}^{\mathsf{T}}$, which requires $\mathbf{DQ}$ to be symmetric, leaves six degrees of freedom. Together with the condition $\operatorname{tr} \mathbf{D} = 0$, there remain five degrees of freedom. Hence, $\mathfrak{D}_{\mathbf{Q}}$ is a *five-dimensional linear space.*

Consider a deformation $\mathbf{D}$ caused by a planar surface optical flow. Substituting $\mathbf{A} = \mathbf{I} + \mathbf{W}\,\Delta t + O(\Delta t^2)$ into $\mathbf{Q}(t + \Delta t) = \mathbf{A}^{-1}\,\mathbf{Q}(t)(\mathbf{A}^{-1})^{\mathsf{T}}$ (proposition 1) and noting that $\mathbf{A}^{-1} = \mathbf{I} - \mathbf{W}\,\Delta t + O(\Delta t^2)$, we obtain

$$\begin{aligned}\mathbf{Q}(t + \Delta t) &= \mathbf{Q}(t) - (\mathbf{W}\,\mathbf{Q}(t) + \mathbf{Q}(t)\mathbf{W}^{\mathsf{T}})\,\Delta t \\ &\quad + O(\Delta t^2) \\ &= [\mathbf{I} - (\mathbf{W} + \mathbf{QW}^{\mathsf{T}}\,\mathbf{Q}^{-1})\,\Delta t \\ &\quad + O(\Delta t^2)]\,\mathbf{Q}(t)\end{aligned} \tag{49}$$

From the definition (47) of the deformation $\mathbf{D}$, we obtain

Proposition 11. The deformation $\mathbf{D}$ of conic $\mathbf{Q}$ caused by optical flow $\mathbf{W}$ is

$$\mathbf{D} = -(\mathbf{W} + \mathbf{QW}^{\mathsf{T}}\,\mathbf{Q}^{-1}) \tag{50}$$

We now prove that $\mathfrak{D}_{\mathbf{Q}}$ is *exactly* the set of all deformations caused by planar surface optical flows.

Proposition 12. The set $\mathfrak{D}_{\mathbf{Q}}$ consists of all deformations of conic $\mathbf{Q}$ caused by optical flows.

Proof: Let $\mathbf{D}$ be a deformation caused by an optical flow $\mathbf{W}$ given by equation (50). Since $\operatorname{tr} \mathbf{W} = 0$, we see that

$$\begin{aligned}\operatorname{tr}\mathbf{D} &= -(\operatorname{tr} \mathbf{W} + \operatorname{tr} \mathbf{QW}^{\mathsf{T}}\,\mathbf{Q}^{-1}) \\ &= -\operatorname{tr} \mathbf{Q}^{-1}\,\mathbf{QW}^{\mathsf{T}} = -\operatorname{tr} \mathbf{W}^{\mathsf{T}} = 0\end{aligned} \tag{51}$$

Also, since both $\mathbf{Q}$ and $\mathbf{Q}^{-1}$ are symmetric, we see that

$$\begin{aligned}\mathbf{DQ} &= -(\mathbf{W} + \mathbf{QW}^{\mathsf{T}}\,\mathbf{Q}^{-1})\,\mathbf{Q} \\ &= -\mathbf{Q}(\mathbf{Q}^{-1}\,\mathbf{WQ} + \mathbf{W}^{\mathsf{T}}) = \mathbf{QD}^{\mathsf{T}}\end{aligned} \tag{52}$$

Hence, $\mathbf{D} \in \mathfrak{D}_{\mathbf{Q}}$. Conversely, we can find for any member $\mathbf{D} \in \mathfrak{D}_{\mathbf{Q}}$ a particular optical flow $\mathbf{W}_0$ that causes deformation $\mathbf{D}$. Indeed, we can choose

$$\mathbf{W}_0 = -\frac{1}{2}\,\mathbf{D} \tag{53}$$

Evidently, $\operatorname{tr} \mathbf{W}_0 = -\operatorname{tr} \mathbf{D}/2 = 0$. Since $\mathbf{QD}^{\mathsf{T}} = \mathbf{DQ}$, we see that

$$\begin{aligned}-(\mathbf{W}_0 + \mathbf{QW}_0^{\mathsf{T}}\,\mathbf{Q}^{-1}) &= -\frac{1}{2}\,(-\mathbf{D} - \mathbf{QD}^{\mathsf{T}}\,\mathbf{Q}^{-1}) \\ &= \frac{1}{2}\,(\mathbf{D} + \mathbf{D}) = \mathbf{D}\end{aligned} \tag{54}$$

This means that the optical flow $\mathbf{W}_0$ causes deformation $\mathbf{D}$ (proposition 11). ■

For a given deformation $\mathbf{D}$, equation (50) is a linear equation in $\mathbf{W}$. Hence, the general solution is given by a particular solution $\mathbf{W}_0$ plus a solution $\mathbf{W}$ of the homogenous equation $-(\mathbf{W} + \mathbf{QW}^{\mathsf{T}}\,\mathbf{Q}^{-1}) = \mathbf{O}$, which is equivalent to $\mathbf{WQ} + \mathbf{QW}^{\mathsf{T}} = \mathbf{O}$. Thus, the set of all homogeneous solutions coincides with the set $h_{\mathbf{Q}}$ of invisible flows (proposition 8), and we obtain proposition 13.

Proposition 13. For every deformation $\mathbf{D} \in \mathfrak{D}_{\mathbf{Q}}$ of conic $\mathbf{Q}$, the general expression of the optical flow $\mathbf{W}$ that causes this deformation is

$$\mathbf{W} = -\frac{1}{2}\,\mathbf{D} + \mathbf{K} \qquad \mathbf{K} \in h_{\mathbf{Q}} \tag{55}$$

The set of all flow matrices is the set $sl(3)$ of all three-dimensional matrixes of trace 0. This is an eight-dimensional linear space with respect to matrix addition and scalar multiplication. Hence, we obtain theorem 1.

Thoerem 1: *The five-dimensional linear space $\mathfrak{D}_{\mathbf{Q}}$ of the deformations of conic $\mathbf{Q}$ is isomorphic to the quotient space of the eight-dimensional linear space $sl(3)$*

of all optical flows modulo the three-dimensional linear space h_Q of invisible flows of **Q**:

$$\mathfrak{D}_Q \cong sl(3)/h_Q \tag{56}$$

Proposition 13 and theorem 1 are a special case of a more general result obtained by Bergholm and Carlsson [2].

Example. Consider the following translating circle:

$$(x - Ut)^2 + (y - Vt)^2 = r^2 \qquad r > 0 \tag{57}$$

The deformation of this conic at $t = 0$ is given as follows:

$$\mathbf{D} = \begin{pmatrix} 0 & 0 & fU/r^2 \\ 0 & 0 & fV/r^2 \\ -U/f & -V/f & 0 \end{pmatrix} \tag{58}$$

The optical flow that causes this deformation has the form

$$\begin{aligned} \dot{x} &= \left(\frac{U}{2} + \frac{c_1 r^2}{f}\right) - \frac{c_3 r^2}{f^2} y \\ &\quad + \left[\left(\frac{U}{2r^2} - \frac{c_1}{f}\right) x + \left(\frac{V}{2r^2} - \frac{c_2}{f}\right) y\right] x \\ \dot{y} &= \left(\frac{V}{2} + \frac{c_2 r^2}{f}\right) + \frac{c_3 r^2}{f^2} x \\ &\quad + \left[\left(\frac{U}{2r^2} - \frac{c_1}{f}\right) x + \left(\frac{V}{2r^2} - \frac{c_2}{f}\right) y\right] y \end{aligned} \tag{59}$$

where c_1, c_2, and c_3 are arbitrary constants. This flow includes, as a special case, the translational flow $\dot{x} = U$ and $\dot{y} = V$ for $c_1 = -fU/2r^2$, $c_2 = -fV/2r^2$, and $c_3 = 0$. ■

9 Contour-Based Optical-Flow Determination

Let C be a contour of general shape at one time, and C' the corresponding contour a short time later. As has been discussed by many researchers [1, 2, 4, 8, 9, 10, 30, 31, 32] the optical flow can be determined from the *normal flow* v_n along the contour without knowing which point corresponds to which (figure 3). This is an advantage, since accurate detection of point correspondences is usually a very difficult task, while

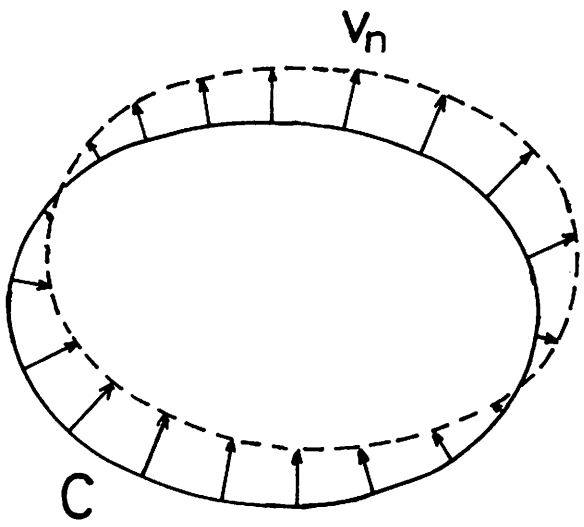

Fig. 3. Image motion of a contour and its normal flow.

contours are generally easily detected by applying an edge operator. In our notation, this is formulated as follows.

Let C be a contour defined by N-vector $\mathbf{m}(s)$ parameterized by arc length s, and let $v_n(s)$ be the normal flow along it. Let $\mathbf{n}(s)$ be the N-vector of the tangent at the point of N-vector $\mathbf{m}(s)$. Let $\mathbf{K} = (0, 0, 1)^\top$.

Proposition 14. Optical flow field $\dot{\mathbf{m}}$ induces the normal flow

$$v_n = \frac{f(\dot{\mathbf{m}}, \mathbf{n})}{(\mathbf{m}, \mathbf{k})\sqrt{1 - (\mathbf{n}, \mathbf{k})^2}} \tag{60}$$

Proof: Consider an image point of N-vector $\mathbf{m}$. From figure 4(a), we see that if its N-velocity is $\dot{\mathbf{m}}$, the image velocity has the form $\mathbf{u} = f\dot{\mathbf{m}}/(\mathbf{m}, \mathbf{k}) + c\mathbf{m}$, where c is a scalar constant. The constant c is determined from the condition $(\mathbf{u}, \mathbf{k}) = 0$, resulting in $c = -f(\dot{\mathbf{m}}, \mathbf{k})/(\mathbf{m}, \mathbf{k})^2$. Hence,

$$\mathbf{u} = \frac{f}{(\mathbf{m}, \mathbf{k})}\left[\dot{\mathbf{m}} - \frac{(\dot{\mathbf{m}}, \mathbf{k})}{(\mathbf{m}, \mathbf{k})}\mathbf{m}\right] \tag{61}$$

From figure 4(b), we see that the unit normal $\mathbf{n}$ to the tangent of N-vector $\mathbf{n}$ on the image plane is given by

$$\tilde{\mathbf{n}} = N[\mathbf{P}_k \mathbf{n}] = \frac{\mathbf{n} - (\mathbf{n}, \mathbf{k})\,\mathbf{k}}{\sqrt{1 - (\mathbf{n}, \mathbf{k})^2}} \tag{62}$$

where $\mathbf{P}_k$ is the orthogonal projection matrix along $\mathbf{k}$ defined by $\mathbf{P}_k = \mathbf{I} - \mathbf{k}\mathbf{k}^\top$. The normal flow v_n is given

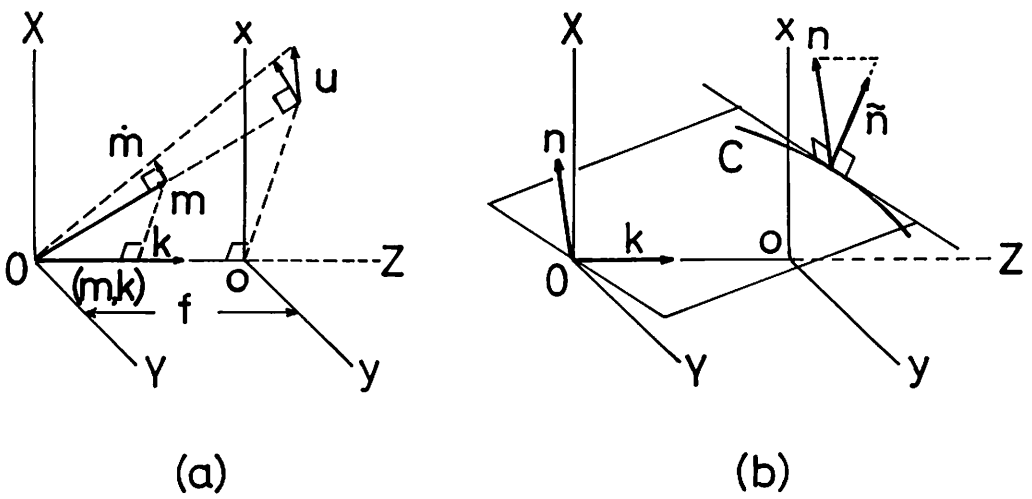

Fig. 4. (a) The N-velocity and the corresponding image velocity. (b) The normal flow along a contour.

by $(\mathbf{u}, \tilde{\mathbf{n}})$. If we note the "incidence equation" $(\mathbf{m}, \mathbf{n}) = 0$ (equation (2)), we obtain equation (60) from equations (61) and (62).

Substituting the flow equation (32) into equation (60) and noting the incidence equation $(\mathbf{m}, \mathbf{n}) = 0$, we obtain the following.

Corollary 3. *Optical flow* $\mathbf{W}$ *induces the normal flow*

$$v_n = \frac{f(\mathbf{m}, \mathbf{Wn})}{(\mathbf{m}, \mathbf{k})\sqrt{1 - (\mathbf{n}, \mathbf{k})^2}} \tag{63}$$

Let us consider the least-squares optimization

$$J = \int_C \left(v_n - \frac{f(\mathbf{m}, \mathbf{Wn})}{(\mathbf{m}, \mathbf{k})\sqrt{1 - (\mathbf{n}, \mathbf{k})^2}} \right)^2 ds \to \min \tag{64}$$

Let us write a tensor $\mathfrak{I} = (T_{ijkl})$ as $\mathfrak{I} = \mathbf{A} \otimes \mathbf{B}$ if it is defined from matrices $\mathbf{A} = (A_{ij})$ and $\mathbf{B} = (B_{ij})$ in the form $T_{ijkl} = A_{ij}B_{kl}$. For a contour C of parameterized N-vector $\mathbf{m}(s)$ having $\mathbf{n}(s)$ as the N-vector of its parameterized tangent, define matrix

$$\mathbf{T}_C(s) = \frac{f\mathbf{m}(s)\mathbf{n}(s)^\mathsf{T}}{(\mathbf{m}(s), \mathbf{k})\sqrt{1 - (\mathbf{n}(s), \mathbf{k})^2}} \tag{65}$$

Proposition 15. The flow matrix $\mathbf{W}$ is determined from a normal flow along a contour C by solving

$$\mathfrak{A}\mathbf{W} = \mathbf{B} \qquad \mathrm{tr}\mathbf{W} = 0 \tag{66}$$

where tensor $\mathfrak{A}$ and matrix $\mathbf{B}$ are defined by

$$\mathfrak{A} = \int_C \mathbf{T}_C(s) \otimes \mathbf{T}_C(s)\, ds$$

$$\mathbf{B} = \int_C v_n(s)\, \mathbf{T}_C(s)\, ds \tag{67}$$

Proof: Note that $(\mathbf{m}, \mathbf{Wn}) = (\mathbf{mn}^\mathsf{T}, \mathbf{W})$, where the left-hand side is the vector inner product, while the right-hand side is the matrix inner product defined by

$$(\mathbf{A}, \mathbf{B}) = \sum_{i,j=1}^{3} A_{ij} B_{ij}.$$

For a perturbation $\mathbf{W} \to \mathbf{W} + \delta\mathbf{W}$, the corresponding first variation of equation (64) is

$$\begin{aligned}\delta J &= -2\int_C \left[v_n(s) - \frac{f(\mathbf{m}(s), \mathbf{Wn}(s))}{(\mathbf{m}(s), \mathbf{k})\sqrt{1 - (\mathbf{n}(s), \mathbf{k})^2} \right] \\ &\quad \times \frac{f(\mathbf{m}(s), \delta\mathbf{Wn}(s))}{(\mathbf{m}(s), \mathbf{k})\sqrt{1 - (\mathbf{n}(s), \mathbf{k})^2}}\, ds \\ &= -2\int_C \left[v_n(s) - \frac{f(\mathbf{m}(s), \mathbf{Wn}(s))}{(\mathbf{m}(s), \mathbf{k})\sqrt{1 - (\mathbf{n}(s), \mathbf{k})^2} \right] \\ &\quad \times \frac{f(\mathbf{m}(s)\ \mathbf{n}(s)^\mathsf{T}}{(\mathbf{m}(s), \mathbf{k})\sqrt{1 - (\mathbf{n}(s), \mathbf{k})^2}}\, ds\ \delta\mathbf{W}\end{aligned} \tag{68}$$

Since this must vanish for any $\delta\mathbf{W}$ such that $\mathrm{tr}\,\delta\mathbf{W} = 0$, we have

$$\int_C \left[v_n(s) - \frac{f(\mathbf{m}(s), \mathbf{W}\mathbf{n}(s))}{(\mathbf{m}(s), \mathbf{k})\sqrt{1 - (\mathbf{n}(s), \mathbf{k})^2}} \right] \times \frac{f(\mathbf{m}(s), \mathbf{n}(s))^\top}{(\mathbf{m}(s), \mathbf{k})\sqrt{1 - (\mathbf{n}(s), \mathbf{k})^2}} ds = c\mathbf{I} \tag{69}$$

where c is a constant. Taking the trace of both sides and noting that tr $(\mathbf{m}(s)\mathbf{n}(s)^\top) = (\mathbf{m}(s), \mathbf{n}(s)) = 0$ (the incidence equation), we obtain $c = 0$ and thereby equations (66) and (67). ■

If we note that tr $\mathbf{T}_C(s) = 0$ due to the incidence equation $(\mathbf{m}(s), \mathbf{n}(s)) = 0$ (see equation (65)), we see that $\mathfrak{A} = (A_{ijkl})$ and $\mathbf{B} = (B_{ij})$ given by (67) satisfy $\Sigma_{i=1}^3 A_{iikl} = 0$ and $\Sigma_{i=1}^3 B_{ii} = 0$, and $\mathfrak{A}\mathbf{W} = \mathbf{B}$ gives only eight independent equations. If the last one is omitted, equations (66) are rearranged in the form of a nine-dimensional vector equations $\hat{\mathbf{A}}\hat{\mathbf{W}} = \hat{\mathbf{B}}$ by defining nine-dimensional vector $\hat{\mathbf{W}} = (W_{11}, W_{12}, \ldots, W_{33})^\top$, nine-dimensional matrix $\hat{\mathbf{A}} = (\hat{A}_{kl})$, $\hat{A}_{11} = A_{1111}, \ldots, \hat{A}_{89} = A_{3233}$, $\hat{A}_{91} = \cdots = \hat{A}_{99} = 1$, and nine-dimensional vector $\hat{\mathbf{B}} = (B_{11}, \ldots, B_{32}, 0)^\top$.

Now, consider the case where the contour C is a conic. The existence of the set $h_\mathbf{Q}$ of invisible flows implies that the optical flow cannot be uniquely determined from the normal flow v_n, because if $\mathbf{W}$ is the optical flow compatible with v_n, so is $\mathbf{W} + \mathbf{K}$ for any $\mathbf{K} \in h_\mathbf{Q}$. This fact was first pointed out by Bergholm [1]. Thus, if tensor $\mathfrak{A}$ is defined by equation (67), any $\mathbf{K} \in h_\mathbf{Q}$ satisfies

$$\mathfrak{A}\mathbf{K} = \mathbf{O} \tag{70}$$

which is easily confirmed (appendix A). However, the deformation $\mathbf{D}$ is uniquely determined from the normal flow v_n along the conic $\mathbf{Q}$:

Proposition 16. The deformation $\mathbf{D}$ of conic $\mathbf{Q}$ is determined from the normal flow v_n along $\mathbf{Q}$ by solving the following linear equations.

$$\mathfrak{A}\mathbf{D} = -2\mathbf{B}, \quad \text{tr } \mathbf{D} = 0, \quad \mathbf{D}\mathbf{Q} = \mathbf{Q}\mathbf{D}^\top \tag{71}$$

where tensor $\mathfrak{A}$ and matrix $\mathbf{B}$ are defined by (67).

Proof: If $\mathbf{D}$ is the deformation of the conic $\mathbf{Q}$, then $\mathbf{W}_0 = -\mathbf{D}/2$ (equation (53)) is a particular optical flow compatible with the deformation, and hence it must satisfy equation (66). Thus, the first of equations (71) is obtained. The second and the third of (71) are the conditions that $\mathbf{D}$ be a deformation of a conic (see (48)). The first of (71) provides eight equations for a matrix of trace 0. The null space of them is simply the space $h_\mathbf{Q}$ of invisible flows, which is three-dimensional (proposition 9). This means that exactly five of the eight equations are linearly independent. Thus, the nine elements of $\mathbf{D}$ are determined uniquely. ■

10 3-D Interpretation of Conic Motion

Suppose the conic we are observing is a perspective projection of a conic in the scene. Let us call the plane on which the conic lies the *supporting plane*. Let $\mathbf{n}$ be its unit surface normal signed so that it points away from the viewpoint O (we do not consider planes passing through the viewpoint O, which are "invisible"). Let d (> 0) be its distance from O. The equation of the plane is $(\mathbf{n}, \mathbf{r}) = d$. Define $\mathbf{p} = \mathbf{n}/d$, and call it the *P-vector* of the plane. Evidently, any plane that does not pass through the viewpoint is uniquely specified by its P-vector: the equation of the plane is $(\mathbf{P}, \mathbf{r}) = 1$.

Suppose the camera is rotated around the viewpoint by $\mathbf{R}$ (rotation matrix) and translated by $\mathbf{h}$ relataive to a planar surface of P-vector $\mathbf{p}$. Let us call the $\{\mathbf{R}, \mathbf{h}\}$ the *motion parameters*. By this camera motion, a collineation is induced on the image plane, because (i) collinear points are mapped to collinear points, (ii) concurrent lines are mapped to concurrent lines, and (iii) the incidence relation is preserved. It is easy to show that the resulting collineation is given by

$$\mathbf{A} = \frac{1}{k}(\mathbf{I} - \mathbf{p}\mathbf{h}^T)\mathbf{R} \qquad k = \sqrt[3]{1 - (\mathbf{p}, \mathbf{h})} \tag{72}$$

and if $\mathbf{A}$ is determined, the motion parameters $\{\mathbf{R}, \mathbf{h}\}$ and the P-vector $\mathbf{p}$ can be computed up to scale and sign. This problem has been studied by many researchers [11, 13, 17, 27, 28, 29].

However, if all we observe is an image motion of a conic $\mathbf{Q}$, the collineation is determined only up to the group $\mathcal{H}_\mathbf{Q}$ of invisible motions, which is a three-dimensional Lie group (section 4). Together with the scale indeterminancy, we need *four additional constraints* to obtain a 3-D interpretation. If we note that the inverse of the collineation $\mathbf{A}$ of equations (72) is

$$\mathbf{A}^{-1} = k\mathbf{R}^\top \left[\mathbf{I} + \frac{\mathbf{p}\mathbf{h}^\top}{1 - (\mathbf{p}, \mathbf{h})} \right] \tag{73}$$

the problem is stated as follows:

Problem 1. Given two conics $\mathbf{Q}$ and $\mathbf{Q}'$ of determinant -1 and signature (2, 1), compute the P-vector

p, the translation **h**, and the rotation matrix **R** that satisfy

$$\mathbf{R}\mathbf{Q}'\mathbf{R}^{\mathsf{T}} = (1 - (\mathbf{p}, \mathbf{h}))^{2/3} \left(\mathbf{I} + \frac{\mathbf{p}\mathbf{h}^{\mathsf{T}}}{1 - (\mathbf{p}, \mathbf{h})} \right) \mathbf{Q} \left(\mathbf{I} + \frac{\mathbf{h}\mathbf{p}^{\mathsf{T}}}{1 - (\mathbf{p}, \mathbf{h})} \right) \tag{74}$$

The number of unknowns is nine (three for **p**, three for **h**, and three for **R**). Since (74) is an equality between two symmetric matrices, it gives *six* equations. However, the determinants are identically -1 on both sides. Hence, only *five* equations are independent, providing five constraints.

Let the right-hand side of equation (74) be $\mathbf{F}(\mathbf{p}, \mathbf{h})$. Let λ_1', λ_2', and λ_3' be the eigenvalues of $\mathbf{Q}'$. There exists an orthogonal matrix $\mathbf{U}'$ that transforms $\mathbf{Q}'$ into its canonical form, that is, $\mathbf{U}'^{\mathsf{T}}\mathbf{Q}'\mathbf{U}' = \mathbf{\Lambda}'$, where $\mathbf{\Lambda}' = \mathrm{diag}(\lambda_1', \lambda_2', \lambda_3')$. Then, (74) is written as

$$\mathbf{R}\mathbf{U}'\mathbf{\Lambda}'(\mathbf{R}\mathbf{U}')^{\mathsf{T}} = \mathbf{F}(\mathbf{p}, \mathbf{h}) \tag{75}$$

Hence, requiring equation (74) is equivalent to requiring matrix $\mathbf{F}(\mathbf{p}, \mathbf{h})$ to have eigenvalues λ_1', λ_2', and λ_3'. If we let $\lambda_1(\mathbf{p}, \mathbf{h})$, $\lambda_2(\mathbf{p}, \mathbf{h})$, and $\lambda_3(\mathbf{p}, \mathbf{h})$ be the eigenvalues of $\mathbf{F}(\mathbf{p}, \mathbf{h})$, and $\mathbf{u}_1(\mathbf{p}, \mathbf{h})$, $\mathbf{u}_2(\mathbf{p}, \mathbf{h})$, and $\mathbf{u}_3(\mathbf{p}, \mathbf{h})$ the corresponding unit eigenvectors, equation (75) splits into three equations

$$\lambda_1(\mathbf{p}, \mathbf{h}) = \lambda_1', \quad \lambda_2(\mathbf{p}, \mathbf{h}) = \lambda_2', \quad \lambda_3(\mathbf{p}, \mathbf{h}) = \lambda_3' \tag{76}$$

Since the products of both sides of these three equations are identically -1, only *two* of these provide independent constraints. Hence, four additional constraints are necessary to determine **p** and **h** as expected.

Equation (75) also states that the three columns of $\mathbf{R}\mathbf{U}'$ are the unit eigenvectors of $\mathbf{F}(\mathbf{p}, \mathbf{h})$. Hence the rotation matrix **R** is determined by

$$\mathbf{R} = (\mathbf{u}_1(\mathbf{p}, \mathbf{h})\ \mathbf{u}_2(\mathbf{p}, \mathbf{h}),\ \mathbf{u}_3(\mathbf{p}, \mathbf{h}))\mathbf{U}'^{\mathsf{T}} \tag{77}$$

Here, $(\mathbf{a}, \mathbf{b}, \mathbf{c})$ denotes the matrix consisting of three columns **a**, **b**, and **c** in that order. There are six ways of ordering the eigenvalues of $\mathbf{F}(\mathbf{p}, \mathbf{h})$ as $\lambda_1(\mathbf{p}, \mathbf{h})$, $\lambda_2(\mathbf{p}, \mathbf{h})$, and $\lambda_3(\mathbf{p}, \mathbf{h})$. Hence, there are *six* sets of equations, yielding at least six sets of solutions for the P-vector **p** and the translation **h**. For each of them, the signs of the eigenvectors are arbitrary except that the determinant of **R** is 1. This gives *four* solutions for **R**, reflecting the axial symmetry of the conic.

11 3-D Interpretation of Conic Deformation

Suppose an infinitesimal motion of conic **Q** is observed. Let **D** be the observed deformation. We now show that the mathematical structure of the information provided by this observation is similar to the case of finite motion. If the camera rotates around the viewpoint with rotation velocity $\boldsymbol{\omega}$ and translates with translation velocity **v** relative to a planar surface of P-vector **p**, it can be shown [11, 13] that the following optical flow is induced on the image plane:

$$\mathbf{W} = \boldsymbol{\omega} \times \mathbf{I} + \frac{1}{3}(\mathbf{p}, \mathbf{v})\mathbf{I} - \mathbf{p}\mathbf{v}^{\mathsf{T}} \tag{78}$$

Here, for matrix $\mathbf{T} = (\mathbf{t}_1, \mathbf{t}_2, \mathbf{t}_3)$ and vector **a**, the symbol $\mathbf{a} \times \mathbf{T}$ denotes the matrix $(\mathbf{a} \times \mathbf{t}_1, \mathbf{a} \times \mathbf{t}_2, \mathbf{a} \times \mathbf{t}_3)$ consisting of vector products of **a** with the columns of **T**. This flow causes the deformation **D** of conic **Q** as stated in proposition 11. Hence, we have the following problem to solve:

Problem 2. Given a conic **Q** of determinant -1 and signature (2, 1) and its deformation **D** of it ($\mathrm{tr}\,\mathbf{D} = 0$, $\mathbf{D}\mathbf{Q} = \mathbf{Q}\mathbf{D}^{\mathsf{T}}$), compute the P-vector **p**, the translation velocity **v**, and the rotation velocity $\boldsymbol{\omega}$ that satisfy

$$\boldsymbol{\omega} \times \mathbf{Q} + (\boldsymbol{\omega} \times \mathbf{Q})^{\mathsf{T}} + \frac{2}{3}(\mathbf{p}, \mathbf{v})\mathbf{Q} - \mathbf{p}(\mathbf{Q}\mathbf{v})^{\mathsf{T}} - (\mathbf{Q}\mathbf{v})\mathbf{p}^{\mathsf{T}} = -\mathbf{D}\mathbf{Q} \tag{79}$$

There exists an orthogonal matrix **U** that transforms **Q** into its canonical form, that is, $\mathbf{U}^{\mathsf{T}}\mathbf{Q}\mathbf{U} = \mathbf{\Lambda}$, where $\mathbf{\Lambda} = \mathrm{diag}(\lambda_1, \lambda_2, \lambda_3)$. If equation (79) is multiplied by $\mathbf{U}^{\mathsf{T}}$ from the left and **U** from the right, we obtain

$$\mathbf{U}^{\mathsf{T}}(\boldsymbol{\omega} \times \mathbf{U})(\mathbf{U}^{\mathsf{T}}\mathbf{Q}\mathbf{U}) + (\mathbf{U}^{\mathsf{T}}\mathbf{Q}\mathbf{U})(\boldsymbol{\omega} \times \mathbf{U})^{\mathsf{T}}\mathbf{U} + \frac{2}{3}(\mathbf{p}, \mathbf{v})\mathbf{U}^{\mathsf{T}}\mathbf{Q}\mathbf{U} - \mathbf{U}^{\mathsf{T}}\mathbf{p}(\mathbf{U}^{\mathsf{T}}\mathbf{Q}\mathbf{U}\mathbf{U}^{\mathsf{T}}\mathbf{v})^{\mathsf{T}} - (\mathbf{U}^{\mathsf{T}}\mathbf{Q}\mathbf{U}\mathbf{U}^{\mathsf{T}}\mathbf{v})(\mathbf{U}^{\mathsf{T}}\mathbf{p})^{\mathsf{T}} = -\mathbf{U}^{\mathsf{T}}\mathbf{D}\mathbf{U}\mathbf{U}^{\mathsf{T}}\mathbf{Q}\mathbf{U} \tag{80}$$

If we define new variables $\mathbf{p}' = \mathbf{U}^{\mathsf{T}}\mathbf{p}$, $\mathbf{v}' = \mathbf{U}^{\mathsf{T}}\mathbf{v}$, and $\boldsymbol{\omega}' = (\det \mathbf{U})\mathbf{U}^{\mathsf{T}}\boldsymbol{\omega}$, and put $\mathbf{D}' = \mathbf{U}^{\mathsf{T}}\mathbf{D}\mathbf{U}$, equation (80) becomes

$$\boldsymbol{\omega}' \times \mathbf{\Lambda} + (\boldsymbol{\omega}' \times \mathbf{\Lambda})^{\mathsf{T}} + \frac{2}{3}(\mathbf{p}', \mathbf{v}')\mathbf{\Lambda} - \mathbf{p}'(\mathbf{\Lambda}\mathbf{v}')^{\mathsf{T}} - (\mathbf{\Lambda}\mathbf{v}')\mathbf{p}'^{\mathsf{T}} = -\mathbf{D}'\mathbf{\Lambda} \tag{81}$$

(Note the identity $\mathbf{U}^{\mathsf{T}}(\boldsymbol{\omega} \times \mathbf{U}) = \mathbf{U}^{\mathsf{T}}(\boldsymbol{\omega} \times \mathbf{I})\mathbf{U} = \det \mathbf{U}(\mathbf{U}^{\mathsf{T}}\boldsymbol{\omega}) \times \mathbf{I}$.) In elements,

$$\begin{bmatrix} 0 & (\lambda_1 - \lambda_2)\omega_3' & (\lambda_3 - \lambda_1)\omega_2' \\ (\lambda_1 - \lambda_2)\omega_3' & 0 & (\lambda_2 - \lambda_3)\omega_1' \\ \lambda_3 - \lambda_1)\omega_2' & (\lambda_2 - \lambda_3)\omega_1' & 0 \end{bmatrix}$$

$$+ \frac{2}{3}(p_1'v_1' + p_2'v_2' + p_3'v_3') \begin{pmatrix} \lambda_1 & & \\ & \lambda_2 & \\ & & \lambda_3 \end{pmatrix}$$

$$- \begin{pmatrix} 2\lambda_1 p_1'v_1' & \lambda_2 p_1'v_2' + \lambda_1 p_2'v_1' & \lambda_3 p_1'v_3' + \lambda_1 p_3'v_1' \\ \lambda_1 p_2'v_1' + \lambda_2 p_1'v_2' & 2\lambda_2 p_2'v_2' & \lambda_3 p_2'v_3' + \lambda_2 p_3'v_2' \\ \lambda_1 p_3'v_1' + \lambda_3 p_1'v_3' & \lambda_2 p_3'v_2' + \lambda_3 p_2'v_3' & 2\lambda_3 p_3'v_3' \end{pmatrix}$$

$$= - \begin{pmatrix} \lambda_1 D_{11}' & \lambda_2 D_{12}' & \lambda_3 D_{13}' \\ \lambda_1 D_{21}' & \lambda_2 D_{22}' & \lambda_3 D_{23}' \\ \lambda_1 D_{31}' & \lambda_2 D_{32}' & \lambda_3 D_{33}' \end{pmatrix} \tag{82}$$

By equating the diagonal elements, we obtain

$$\begin{aligned} -2p_1'v_1' + p_2'v_2' + p_3'v_3' &= -\frac{3}{2} D_{11}' \\ p_1'v_1' - 2p_2'v_2' + p_3'v'_3 &= -\frac{3}{2} D_{22}' \\ p_1'v_1' + p_2'v_2' - 2p_3'v'_3 &= -\frac{3}{2} D_{33}' \end{aligned} \tag{83}$$

Since tr $\mathbf{D}' = \text{tr}\,(\mathbf{U}^\top\mathbf{D}\mathbf{U}) = \text{tr}\,\mathbf{D} = 0$, the sums of both sides of the three equations are identically 0. Hence, only *two* of these are independent, providing two constraints. This means that four additional constraints are necessary to determine $\mathbf{p}'$ and $\mathbf{v}'$, as expected.

Equations (83) are equivalently rewritten as

$$\begin{aligned} p_1'v_1' &= \frac{1}{2} D'_{11} + c \\ p_2'v_2' &= \frac{1}{2} D'_{22} + c \\ p_3'v_3' &= \frac{1}{2} D'_{33} + c \end{aligned} \tag{84}$$

where c is an arbitrary constant. Equating the off-diagonal elements of equation (82), we obtain

$$\begin{aligned} (\lambda_2 - \lambda_3)\omega_1' &= \lambda_2 p_3'v_2' + \lambda_3 p_2'v_3' - \lambda_3 D_{23}' \\ (\lambda_3 - \lambda_1)\omega_2' &= \lambda_3 p_1'v_3' + \lambda_1 p_3'v_1' - \lambda_1 D_{31}' \\ (\lambda_1 - \lambda_3)\omega_3' &= \lambda_1 p_2'v_1' + \lambda_2 p_1'v_2' - \lambda_2 D_{12}' \end{aligned} \tag{85}$$

Hence, if the three eigenvalues of $\mathbf{Q}$ are distance, vector ω' is uniquely determined in terms of $\mathbf{p}'$ and $\mathbf{v}'$. If $\mathbf{p}'$, $\mathbf{v}'$, and ω' are determined, the original variables are given by $\mathbf{p} = \mathbf{U}\mathbf{p}'$, $\mathbf{v} = \mathbf{U}\mathbf{v}'$, and $\omega = (\det \mathbf{U})\mathbf{U}\omega'$.

Indeterminancy occurs if any two of λ_1, λ_2, and λ_3 coincide. If $\lambda_1 = \lambda_2$, for example, the axial symmetry around the third axis leaves the angular velocity ω_3' interdeterminate.

12 Conic Stereo

We have shown that four constraints are necessary to compute the 3-D structure and motion from conic motion. We consider a practical method for resolving this ambiguity. Suppose the motion parameters $\{\mathbf{R}, \mathbf{h}\}$ are known. This situation arises when we view a conic placed in the scene by two cameras, whose relative position is specified by the (known) motion parameters $\{\mathbf{R}, \mathbf{h}\}$ of the second camera relative to the first camera (figure 5). We call this problem *conic stereo.*

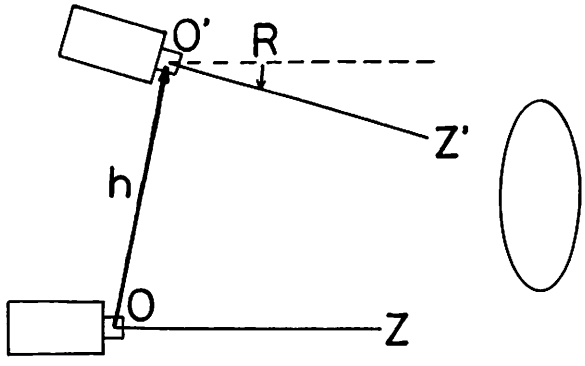

Fig. 5. Conic stereo.

In usual stereo, we must first seek point-to-point correspondences between the two images. In conic stereo, however, the 3-D position and orientation of the conic can be computed without detecting point-to-point correspondences: all we need is a conic-to-conic correspondence. Of course, if a conic-to-conic correspondence is available, point-to-point correspondences can be computed by applying the "epipolar constraint" assigned by the 3-D camera configuration. However, what can be computed from point-to-point correspondences is the *depths* of the individual points. In order to compute the 3-D position and orientation of the conic, a planar surface must be fitted to the computed depths. But this can be done directly from the original conics themselves. Since conics are very prominent features, it is not difficult to establish a correspondence between conics. Indeed, the subsequent method itself can be used to establish correct conic-to-conic correspondences, as will be mentioned shortly. If the

scene (or the camera) is moving continuously, we can also make use of the technique called "snake" to follow a moving conic continuously on the image plane.

Since the motion parameters $\{\mathbf{R}, \mathbf{h}\}$ have *six* degrees of freedom, the problem is now *overspecification*. Equation (74) is rewritten as

$$(\mathbf{I} - \mathbf{ph}^\mathsf{T})\mathbf{RQ}^\mathsf{T}\mathbf{R}^\mathsf{T}(\mathbf{I} - \mathbf{hp}^\mathsf{T}) = (1 - (\mathbf{p}, \mathbf{h}))^{2/3}\mathbf{Q} \quad (86)$$

If ratios of element-wise equations are taken, the factor $(1 - (\mathbf{p}, \mathbf{h}))^{2/3}$ can be eliminated, and we obtain polynomials of second degree in $\mathbf{p}$. If three of them are chosen, the value of $\mathbf{p}$ can be determined. However, it is more realistic to take advantage of this redundancy to increase robustness by means of optimization. Consider the least-square optimization.

$$J(\mathbf{p}) = \|(\mathbf{I} - ph^\mathsf{T})\mathbf{RQ}^\mathsf{T}\mathbf{R}^\mathsf{T}(\mathbf{I} - \mathbf{hp}^\mathsf{T}) - (1 - (\mathbf{p}, \mathbf{h}))^{2/3}\,\mathbf{Q}\|^2 \to \min \quad (87)$$

where $\|\cdot\|$ denotes matrix norm:

$$\|\mathbf{Q}\|^2 = \sum_{i,j=1}^{3} Q_{ij}^2 \; (= \operatorname{tr} \mathbf{Q}^2) \qquad \text{for } \mathbf{Q} = (Q_{ij}).$$

This is nonlinear optimization, so numerical search is necessary. In doing numerical search, two problems emerge:

1. In order that the search is not trapped into a local minimum, a good initial guess must be given in the vicinity of the true solution. How can we obtain one?
2. In order to use a library routine (e.g., the quasi-Newton method [20]), the gradient $\nabla J(\mathbf{p})$ of the cost function $J(\mathbf{p})$ must be given, but its analytical form is difficult to derive.

The first problem can be solved by adopting the "optical flow approximation" described in the preceding section. Namely, if the second image is regarded as obtained after one second, the image motion can be regarded as a flow with instantaneous motion parameters $\boldsymbol{\omega} \approx \Omega\mathbf{l}$ and $\mathbf{v} \approx \mathbf{h}$, where Ω and $\mathbf{l}$ are, respectively, the angle and axis (unit vector) of rotation $\mathbf{R}$. Then, the P-vector $\mathbf{p}$ satisfies equation (79), where the term $\mathbf{DQ}$ on the right-hand side is approximated by $\mathbf{DQ} \approx \mathbf{Q}' - \mathbf{Q}$. Since (79) is also overspecification for $\mathbf{p}$, we consider the least-squares optimization

$$\hat{J}(\mathbf{p}) = \|\boldsymbol{\omega} \times \mathbf{Q} + (\boldsymbol{\omega} \times \mathbf{Q})^\mathsf{T} + \frac{2}{3}(\mathbf{p}, \mathbf{v})\mathbf{Q} - \mathbf{p}(\mathbf{Qv})^\mathsf{T} - (\mathbf{Qv})\mathbf{p}^\mathsf{T} + \mathbf{DQ}\| \to \min \quad (88)$$

Differentiating $\hat{J}(\mathbf{p})$ with respect to each component of $\mathbf{p}$ and setting the result to 0, we obtain the following linear equation:

$$\mathbf{Tp} = \mathbf{b} \quad (89)$$

Here, the matrix $\mathbf{T}$ and the vector $\mathbf{b}$ are given by

$$\mathbf{T} = \frac{4}{9}\|\mathbf{Q}\|^2\mathbf{vv}^\mathsf{T} - \frac{4}{3}(\mathbf{Quv}^\mathsf{T} + \mathbf{vu}^\mathsf{T}\mathbf{Q}) + 2(\mathbf{uu}^\mathsf{T} + \|\mathbf{u}\|^2\mathbf{I}) \quad (90)$$

$$\mathbf{b} = 2\mathbf{Su} - \frac{2}{3}(\mathbf{S}, \mathbf{Q}) \quad (91)$$

where

$$\mathbf{u} = \mathbf{Qv} \qquad \mathbf{S} = \mathbf{DQ} + \boldsymbol{\omega} \times \mathbf{Q} + (\boldsymbol{\omega} \times \mathbf{Q})^\mathsf{T} \quad (92)$$

and $(\mathbf{S}, \mathbf{Q})$ is the matrix inner product of $\mathbf{S}$ and $\mathbf{Q}$ (see equation (68)). An initial estimate is given by solving equation (89). A better approximation is obtained if $\boldsymbol{\omega} \times \mathbf{Q} + (\boldsymbol{\omega} \times \mathbf{Q})^\mathsf{T}$ in (92) is replaced by $\mathbf{RQ} - \mathbf{QR}$.

The problem of computing the gradient can be solved by using *automatic differentiation software* [7], which generates a program for computing $\nabla J(\mathbf{p})$ from a program for computing $J(\mathbf{p})$. In our experiment, we used a system named ADDS developed by Yoshida [33].

Thus, once a correct conic-to-conic corespondence is given, the P-vector of the supporting plane can be robustly determined, and the residual $J(\mathbf{p})$ of equation (87) should be close to zero. If the assumed correspondence is wrong, it is incompatible with equation (86), so the residual $J(\mathbf{p})$ should be large. This means that the residual $J(\mathbf{p})$ can be used as the matching criterion of conics, as pointed out by Ma et al. [18].

Example. Figures 6(a) and (b) show conics computed from real images (512 × 512 pixels) taken by two different cameras (of different focal lengths). We applied the Sobel edge operator and manually chose conic edge segments, to each of which the matrix representation $\mathbf{Q}$ was computed. Many studies have been done about conic fitting techniques [3, 5, 14, 19, 22, 25]; here, we applied the method described in [14]. We must also calibrate the focal lengths f and f' (for (a) and (b), respectively) and the motion parameters $\{\mathbf{R}, \mathbf{h}\}$. They are computed by using a square grid pattern also shown in the same pictures—we followed the computational procedures described in [12, 16]. In this case, $f = 1178$ (pixels) and $f' = 1906$ (pixels). The angle and axis (unit vector) of the rotation $\mathbf{R}$ are 25.6° (−0.831, 0.265, 0.488), respectively, and the translation is $\mathbf{h} = (-9.67, -41.67,$

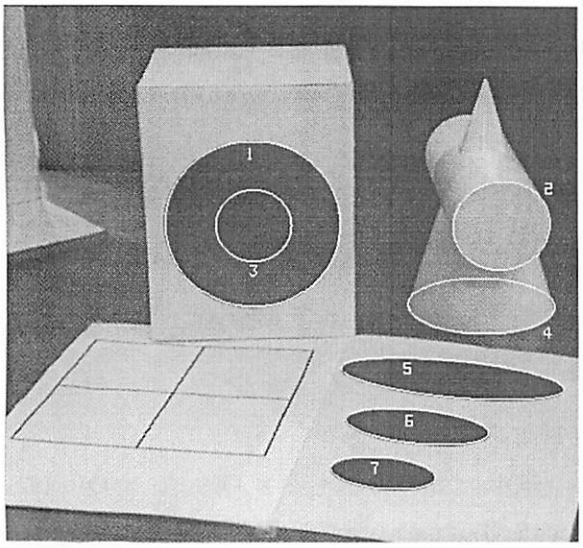

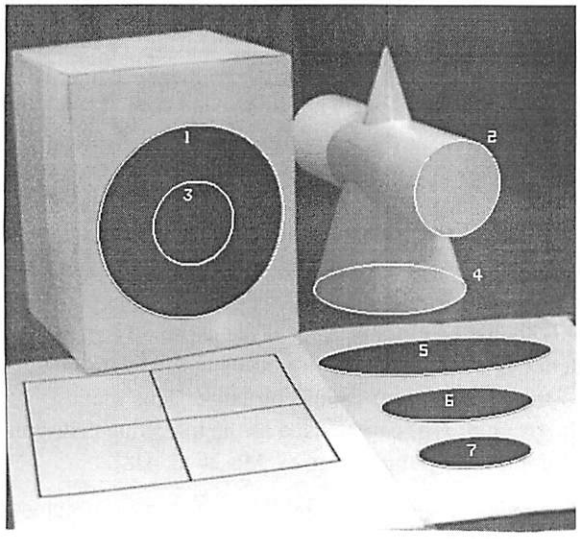

Fig. 6. Conics computed from real images taken by two different cameras.

$-9.95)^\top$ (in cm), respectively. Then, we computed the unit surface normal $\mathbf{n}$ and the distance d (cm) to the supporting planes for the seven conics numbered in the images by manually specifying their correspondences. Table 1 lists the result.

We observe that conics on the same object surface give approximately the same supporting planes; the maximum error in the orientation of the surface normal is about 2.6°. However, errors are large for conics on coplanar but different object surfaces (about 7–10° errors in orientation). This is probably due to inaccurate calibration of the two cameras and distortions of the images. As predicted, the use of a partial conic (conic 4 in the figures) gives poorer results than do complete conics. ■

Table 1. The unit surface normal $\mathbf{n}$ and the distance d to the supporting plane.

	$\mathbf{n}$			d
1	(0.350,	−0.070,	0.934)	90.0
2	(0.435,	−0.145,	0.889)	83.7
3	(0.338,	−0.079,	0.938)	90.3
4	(−0.911,	−0.147,	0.386)	43.7
5	(−0.866,	−0.210,	0.455)	50.4
6	(−0.856,	−0.203,	0.475)	52.1
7	(−0.850,	−0.188,	0.492)	53.4

13 Circular Pattern Projection

As another application, we replace the second camera of conic stereo (figure 5) by a spot light source that emits a circular light pattern (figure 7(a)). This is equivalent to the second camera in figure 5 observing an image of a circle $\mathbf{Q}'$.

The light source does not have an image plane, but the representation $\mathbf{Q}'$ of the circle is easily obtained by a prior calibration. If the orientation of the light source is adjusted relative to a planar surface in the scene so that a circle is projected onto it, the planar surface can be regarded as a hypothetical "image plane" of the light source. Let r_1 be the radius of the circular pattern on it, and let r_2 be the radius of the circular pattern after the planar surface is translated away from the camera by d (figure 7(b)). Then, the hypothetical "focal length" of the light source is

$$f = \frac{r_1 d}{r_2 - r_1} \tag{93}$$

and the circle is represented by matrix

$$\mathbf{Q}' = \kappa' \begin{pmatrix} 1 & & \\ & 1 & \\ & & -r_1^2/f^2 \end{pmatrix} \tag{94}$$

where $\kappa' = (f/r_1)^{2/3}$. Note that the representation $\mathbf{Q}'$ is "intrinsic" to the light source independent of the location and orientation (or even *existence*) of the planar surface.

Example. We made a slide film of a circular pattern and projected it onto a planar surface in the scene by a slide projector. Figure 8 shows three images for different

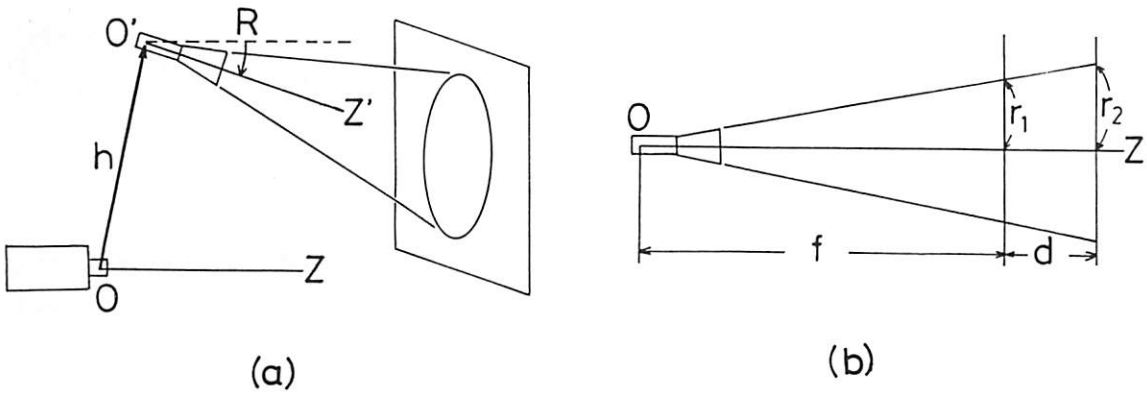

Fig. 7. (a) Circular light pattern projection. (b) Calibration of the light source.

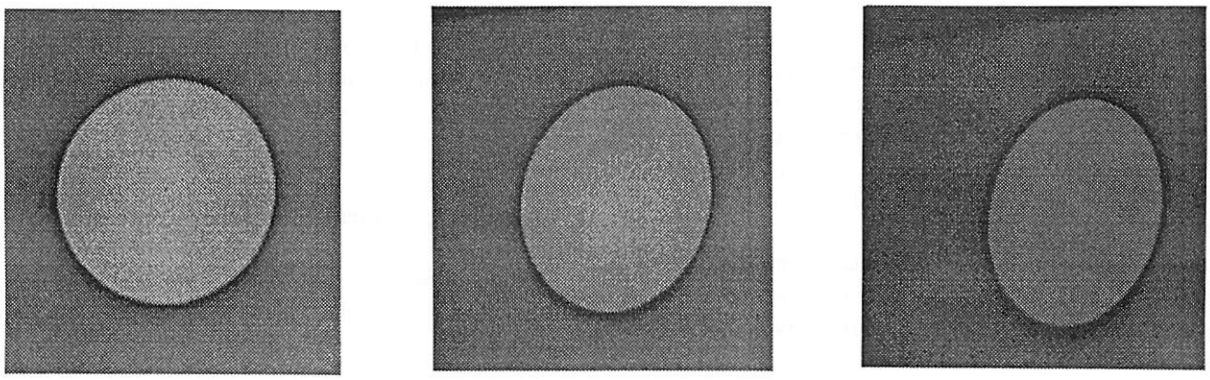

Fig. 8. Real images of a circular pattern in scene.

orientations of the planar surface. The unit surface normal **n** and the distance d (cm) to the surface were computed in each case as shown in table 2. The three planes were arranged so that those in (a) and (b) made angle 30° and those in (a) and (c) made angle 45°. Their computed values are 30° and 48°, respectively.

Table 2. The unit surface normal **n** and the distance d to the planar surface.

	n			d
(a)	(−0.023,	0.218,	0.976)	240.1
(b)	(0.206,	0.632,	0.747)	204.3
(c)	(0.308,	0.801,	0.513)	161.3

The motion parameters $\{\mathbf{R}, \mathbf{h}\}$ of the light source relative to the camera were calibrated beforehand. We made a slide film of a square grid pattern and projected it onto a planar surface whose orientation was adjusted so that an exact square grid pattern was projected onto it (figure 9(a)). If this planar surface is regarded as a hypothetical image plane of the light source, the N-vector $\mathbf{m}'_\alpha$ of each of the vertices can be computed with respect to the light source. The hypothetical focal length is determined by the method described earlier.

From the image taken by the camera (figure 9(b)), the N-vectors $\{\mathbf{m}_\alpha\}$ of corresponding vertices are computed with respect to the camera. The collineation **A** that relates the two (hypothetical and real) "images" are computed from the N-vectors $\{\mathbf{m}_\alpha\}$ and $\{\mathbf{m}'_\alpha\}$ (appendix B). From it, the motion parameters $\{\mathbf{R}, \mathbf{h}\}$ and the P-vector **p** of the planar surface with respect to the camera are computed by the analytical procedure [11, 13]. The absolute scale is easily computed (appendix C). ■

It appears that this calibration can be done away if the square grid pattern is projected onto an unknown planar surface from the beginning. However, we then

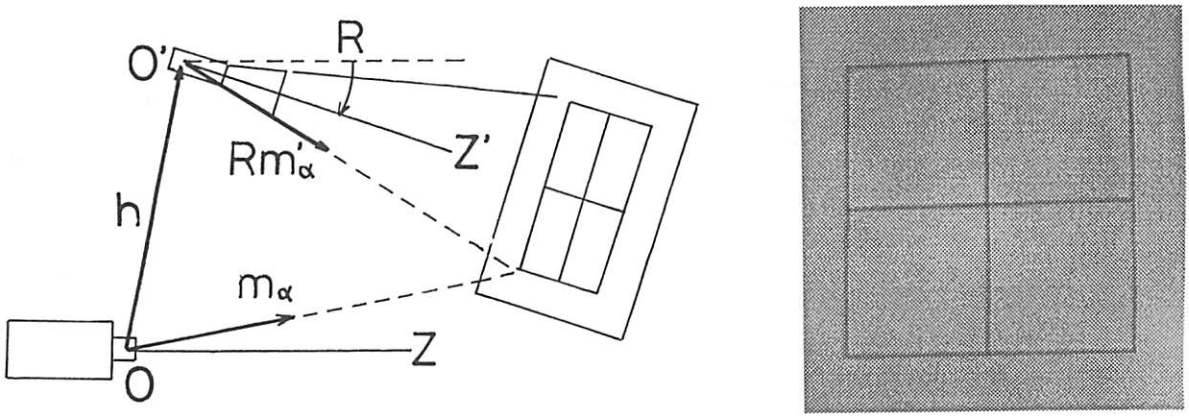

Fig. 9. (a) Calibration of the light source by projecting a square grid pattern. (b) A real image of a projected square grid pattern.

have to find correspondences of the vertices between the original pattern and the camera image. This is difficult when the 3-D position and orientation of the planar surface are unknown. Also, the camera image may not contain all the vertices. If a circular pattern is used, we need not find point-to-point correspondences. Also, even if a partial conic is observed, its matrix representation is easily obtained by conic fitting (although accuracy may decrease). Thus, the use of a circular pattern provides more flexibility at the cost of prior calibration.

14 Concluding Remarks

We have presented a complete analysis of the intrinsic indeterminacy of conic motion by invoking Lie group theory [10] and defining such concepts as groups of invisible motion, their isomorphisms, the standard circle, the Lorentz group, spaces of invisible optical flows, and quotient spaces. We also discussed the relationships to 3-D interpretation and presented two practical applications: computing the 3-D position and orientation of a conic in the scene by two cameras; computing the 3-D position and orientation of a planar surface by using one camera and projecting a circular light pattern. From our real-image experiment, these techniques seem very promising when used in industrial environments.

Acknowledgments

The authors thank Dr. Azriel Rosenfeld of the University of Maryland for detailed discussions on this research. They also thank Dr. Toshinobu Yoshida of the University of Electrocommunications, Japan, for providing us with the automatic differentiation software ADDS whch he himself had developed.

Appendix A: Optical Flow from Contour

Proposition A.1. Let $\mathbf{T}_C(s)$ be the matrix defined by equation (65) for the contour C of conic $\mathbf{Q}$. An optical flow $\mathbf{W}$, tr $\mathbf{W} = 0$, satisfies

$$(\mathbf{T}_C(s) \otimes \mathbf{T}_C(s))W = \mathbf{O} \tag{95}$$

for all s if and only if

$$\mathbf{WQ} + \mathbf{QW}^\mathsf{T} = \mathbf{O} \tag{96}$$

Proof: From equation (65), the equation $(\mathbf{T}_C(s) \otimes \mathbf{T}_C(s))\mathbf{W} = \mathbf{O}$ is equivalent to

$$(\mathbf{m}(s),\ \mathbf{W}n(s)) = 0 \tag{97}$$

A tangent to a conic is the "polar" of the tangent point. It can be proved that the N-vector $\mathbf{n}(s)$ of the tangent to conic $\mathbf{Q}$ at the point of N-vector $\mathbf{m}(s)$ is given by $\mathbf{n}(s) = \pm N[\mathbf{Qm}(s)]$ [13, 26]. Hence, the above equation is equivalent to

$$(\mathbf{m}(s),\ \mathbf{WQm}(s)) = 0. \tag{98}$$

This is a quadratic form in $\mathbf{m}(s)$, so only the symmetric part of $\mathbf{WQ}$ is constrained. Hence, the above equation is equivalent to

$$(\mathbf{m},\ (\mathbf{WQ} + \mathbf{QW}^\mathsf{T})\mathbf{m}) = 0 \tag{99}$$

This equation is satisfied by all $\mathbf{m}$ such that $(\mathbf{m}, \mathbf{Qm}) = 0$ if and only if there exists a constant c such that

$$\mathbf{WQ} + \mathbf{QW}^{\mathrm{T}} = c\mathbf{Q} \tag{100}$$

Multiplying this equation by $\mathbf{Q}^{-1}$ from left, we have

$$\mathbf{Q}^{-1}\mathbf{WQ} + \mathbf{W} = c\mathbf{I} \tag{101}$$

Taking the trace of both sides and noting that tr $(\mathbf{Q}^{-1}\mathbf{WQ})$ = tr $(\mathbf{QQ}^{-1}\mathbf{W})$ = tr $\mathbf{W}$ = 0, we find that $c = 0$. Hence, the proposition is obtained. ■

Appendix B: Determination of Collineation

Given two sets of points $\{P_\alpha\}$ and $\{P'_\alpha\}$, $\alpha = 1, \ldots, N$, on the image plane, the collineation that maps each P_α to P'_α is computed as follows. Let $\{\mathbf{m}_\alpha\}$ and $\{\mathbf{m}'_\alpha\}$ be their respective N-vectors. The problem is to find a matrix $\mathbf{A}$, det $\mathbf{A} = 1$, such that $N[\mathbf{A}^{\mathrm{T}}\mathbf{m}_\alpha] = \mathbf{m}'_\alpha$, $\alpha = 1, \ldots, N$.

Let h_α be the distance of the end point of vector $\mathbf{A}^{\mathrm{T}}\mathbf{m}_\alpha$ from the line that passes through the viewpoint O and extends in the direction of $\mathbf{m}'_\alpha$. From figure B.1, we see that

$$h_\alpha^2 = \|\mathbf{A}^{\mathrm{T}}\mathbf{m}_\alpha\|^2 - (\mathbf{m}'_\alpha, \mathbf{A}^{\mathrm{T}}\mathbf{m}_\alpha)^2 \tag{102}$$

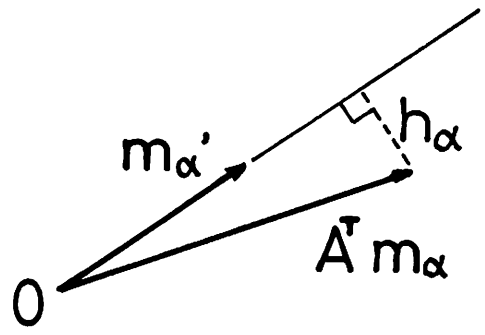

Fig. B.1. The distance of the end point of $\mathbf{A}^{\mathrm{T}}\mathbf{m}_\alpha$ from the line defined by $\mathbf{m}'_\alpha$.

Hence, $\mathbf{A}$ is robustly computed by the least-squares optimization

$$\sum_{\alpha=1}^{N} [\|\mathbf{A}^{\mathrm{T}}\mathbf{m}_\alpha\|^2 - (\mathbf{m}'_\alpha, \mathbf{A}^{\mathrm{T}}\mathbf{m}_\alpha)^2] \rightarrow \min \tag{103}$$

Instead of assigning the constraint det $\mathbf{A} = 1$, we compute the solution under the constraint $\|\mathbf{A}\| = 1$ and then rescale $\mathbf{A}$ so that det $\mathbf{A} = 1$. Let $\mathbf{M} = (M_{ij})$ be the *moment matrix* of $\{\mathbf{m}_\alpha\}$:

$$\mathbf{M} = \sum_{\alpha=1}^{N} \mathbf{m}_\alpha \mathbf{m}_\alpha^{\mathrm{T}} \tag{104}$$

Define the *correlation tensor* $\mathfrak{M} = (M_{ijkl})$ by

$$M_{ijkl} = \sum_{\alpha=1}^{N} m_{\alpha(i)} m'_{\alpha(j)} m_{\alpha(k)} m'_{\alpha(l)} \tag{105}$$

where $m_{\alpha(i)}$ and $m'_{\alpha(i)}$ are the ith components of vectors $\mathbf{m}_\alpha$ and $\mathbf{m}'_\alpha$, respectively. Then, define a tensor $\mathfrak{T} = (T_{ijkl})$ by

$$T_{ijkl} = M_{ik}\delta_{jl} - M_{ijkl} \tag{106}$$

which determines a linear mapping from a matrix to a matrix: $\mathfrak{T}\mathbf{A}$ is the matrix whose (ij) element is $\Sigma_{k,l=1}^{3} T_{ijkl} A_{kl}$. The optimization (103) is written as

$$\sum_{i,j,k,l=1}^{3} T_{ijkl} A_{ij} A_{kl} \rightarrow \min \qquad \sum_{i,j=1}^{3} A_{ij}^2 = 1 \tag{107}$$

If a nine-dimensional vector $\hat{\mathbf{A}} = (\hat{A}_\kappa)$ is defined by renaming indices (i, j) as $\kappa = 3(i-1) + j$, and a nine-dimensional matrix $\hat{\mathbf{T}} = (\hat{T}_{\kappa\lambda})$ by renaming two pairs of indices (i, j) and (k, l) as $(\kappa, \lambda) = (3(i-1) + j, 3(k-1) + l)$, the above minimization now reads

$$\sum_{\kappa,\lambda=1}^{9} \hat{T}_{\kappa\lambda} \hat{A}_\kappa \hat{A}_\lambda \rightarrow \min \qquad \sum_{\kappa=1}^{9} \hat{A}_\kappa^2 = 1 \tag{108}$$

The minimum is attained by the nine-dimensional unit eigenvector $\hat{\mathbf{A}}$ of matrix $\hat{\mathbf{T}}$ for the smallest eigenvalue. The computed nine-dimensional vector $\hat{\mathbf{A}} = (\hat{A}_\kappa)$ is then rearranged into a three-dimensional matrix $\mathbf{A} = (A_{ij})$ by renaming the index κ back to $i = (\kappa - 1)$ div $3 + 1$ and $j = (\kappa - 1) \bmod 3 + 1$, where the operator "div" means the integer part of the quotient, and the operator "mod" means the remainder.

Appendix C: Determination of Scale

Let A and B be points on a planar surface whose unit surface normal is $\mathbf{n}$. Let $\mathbf{m}_A$ and $\mathbf{m}_B$ be their respective N-vectors. If the distance between points A and B is w, the distance d to the planar surface from the viewpoint O is given by

$$d = w \Big/ \left\| \frac{\mathbf{m}_A}{(\mathbf{n}, \mathbf{m}_A)} - \frac{\mathbf{m}_B}{(\mathbf{n}, \mathbf{m}_B)} \right\| \tag{109}$$

This is derived as follows. If $\vec{OA} = r_A\mathbf{m}_A$ and $\vec{OB} = r_B\mathbf{m}_B$, then $d = |(\mathbf{n}, \vec{OA})| = r_A(\mathbf{n}, \mathbf{m}_A)$. Now, $\vec{BA} = r_A\mathbf{m}_A - r_B\mathbf{m}_B$, which is orthogonal to $\mathbf{n}$. Hence,

$$(\mathbf{n}, \vec{BA}) = r_A(\mathbf{n}, \mathbf{m}_A) - r_B(\mathbf{n}, \mathbf{m}_B) = 0 \quad (110)$$

from which we obtain

$$\vec{BA} = r_A\left(\mathbf{m}_A - \frac{(\mathbf{n}, \mathbf{m}_A)}{(\mathbf{n}, \mathbf{m}_B)}\mathbf{m}_B\right)$$

$$= r_A(\mathbf{n}, \mathbf{m}_A)\left(\frac{\mathbf{m}_A}{(\mathbf{n}, \mathbf{m}_A)} - \frac{\mathbf{m}_B}{(\mathbf{n}, \mathbf{m}_B)}\right) \quad (111)$$

Hence, $d = \|\vec{BA}\|/\|\mathbf{m}_A/(\mathbf{n}, \mathbf{m}_A) - \mathbf{m}_B/(\mathbf{n}, \mathbf{m}_B)\|$. From $\|\vec{BA}\| = w$, we obtain equation (109).

Let $\mathbf{p}$ be the P-vector of the planar surface computed by assuming that the camera translation $\mathbf{h}$ is a unit vector. This means that the distance to the planar surface is $1/\|\mathbf{p}\|$. If the true distance to the planar surface is d, the interpretation must be scaled accordingly, and the true P-vector $\bar{\mathbf{p}}$ and the true translation $\bar{\mathbf{h}}$ are respectively given by

$$\bar{\mathbf{p}} = \frac{1}{d}N[\mathbf{p}] \qquad \bar{\mathbf{h}} = d\|\mathbf{p}\|h \quad (112)$$

References

1. F. Bergholm, Motion from flow along contours: A note on robustness and ambiguous cases, *Intern. J. Comput. Vis.* 4: 395–415, 1989.
2. F. Bergholm and S. Carlsson. A "theory" of optical flow, *Comput. Vis. Graph. Image Process.: Image Understanding* 53: 171–188, 1991.
3. F.L. Bookstein, Fitting conic sections to scattered data, *Comput. Graph. Image Process.* 9: 56–71, 1979.
4. L.S. Davis, Z. Wu, and H. Sun, Contour-based motion estimation, *Comput. Vis. Graph. Image Process.* 33: 313–326, 1983.
5. T. Ellis, A. Abboot, and B. Brillault, Ellipse detection and matching with uncertainty, *Image Vis. Comput.* 10: 271–276, 1992.
6. D. Forsyth, J.L. Mundy, A. Zisserman, C. Coelho, A. Heller, and C. Rothwell, Invariant descriptors for 3-D object recognition and pose, *IEEE Trans. Patt. Anal. Mach. Intell.* 13: 971–991, 1991.
7. A. Griewank and G.F. Corliss (eds.), *Automatic Differentiation of Algorithms: Theory, Implementation, and Application*. Soc. for Indust. and Applied Mathematics: Philadelphia, PA, 1991.
8. K. Kanatani, Tracing planar surface motion from a projection without knowing correspondence, *Comput. Vis. Graph. Image Process.* 29: 1–12, 1985.
9. K. Kanatani, Detecting the motion of a planar surface by line and surface integrals, *Comput. Vis. Graph. Image Process.* 29: 13–22, 1985.
10. K. Kanatani, *Group-Theoretical Methods in Image Understanding*. Springer: Berlin, 1990.
11. K. Kanatani, Computational projective geometry, *Comput. Vis. Graph. Image Process.: Image Understanding* 54: 333–348, 1991.
12. K. Kanatani, Statistical analysis of focal-length calibration using vanishing points, *IEEE Trans. Robot. Autom.* 8(6): 1992 (to appear).
13. K. Kanatani, *Geometric Computation for Machine Vision*. Oxford Univ. Press: Oxford, 1993.
14. K. Kanatani, Statistical bias of conic fitting and renormalization, *IEEE Trans. Patt. Anal. Mach. Intell.* 15(1): 1993 (to appear).
15. K. Kanatani and W. Liu, 3-D interpretation of conics and orthogonality, *Comput. Vis. Graph. Image Process.: Image Understanding* (to appear).
16. K. Kanatani and Y. Onodera, Anatomy of camera calibration using vanishing points, *IEICE Trans. Infor. Sys.* 74(10): 3369–3378, 1991.
17. H.C. Longuet-Higgins, The reconstruction of a plane surface from two perspective projections, *Proc. Roy. Soc.* London B-227: 399–410, 1986.
18. S.D. Ma, S.H. Si, and Z.Y. Chen, Quadric curve based stereo, *Proc. 11th Intern. Conf. Patt. Recog.*, August–September, the Hague, the Netherlands, vol. 1, pp. 1–4, 1992.
19. J. Porrill, Fitting ellipses and predicting confidence envelopes using a bias corrected Kalman filter, *Image Vis. Comput.* 8: 37–51, 1990.
20. W.H. Press, B.P. Flannery, S.A. Teukolsky, and W.T. Vetterling, *Numerical Recipes in C*. Cambridge Univ. Press: Cambridge, 1988.
21. C.A. Rothwell, A. Zisserman, C.I. Marinos, D.A. Forsyth, and J.L. Mundy, Relative motion and pose from arbitrary plane curves. *Image Vis. Comput.* 10(4): 250–262, 1992.
22. R. Safaee-Rad, I. Tchoukanov, B. Benhabib, and K.C. Smith, Accurate parameter estimation of quadratic curves from grey-level images. *Comput. Vis. Graph. Image Process.: Image Understanding* 54: 259–274, 1991.
23. R. Safaee-Rad, I. Tchoukanov, K.C. Smith, and B. Benhabib, Constraints on quadratic-curved features under perspective projection, *Image Vis. Comput.* 19(8): 532–548, 1992.
24. R. Safaee-Rad, I. Tchoukanov, K.C. Smith, and B. Benhabib, Three-dimensional location estimation of circular features for machine vision, *IEEE Trans. Robot. Autom.* 8(5): 624–640, 1992.
25. P.D. Sampson, Fitting conic sections to "very scattered" data: An iterative refinement of the Bookstein algorithm, *Comput. Graph. Image Process.* 18: 97–108, 1982.
26. J.G. Semple and G.T. Kneebone, *Algebraic Projective Geometry*. Clarendon Press: Oxford, 1952 (reprinted 1979).
27. R.Y. Tsai and T.S. Huang, Estimating three-dimensional motion parameters of rigid planar patch, *IEEE Trans. Acoust. Speech Sig. Process.* 29: 1147–1152, 1981.
28. T.Y. Tsai and T.S. Huang, Estimating 3-D motion parameters of a rigid planar patch III. Finite point correspondences and the three-view problem, *IEEE Trans. Acoust. Speech Sig. Process.* 32: 213–220, 1984.
29. R.Y. Tsai, T.S. Huang, and W.-L. Zhu, Estimating three-dimensional motion parameters of a rigid planar patch, II: Singular value decomposition, *IEEE Trans. Acoust. Speech Sig. Process.* 30: 525–534, 1982.
30. A.M. Waxman and K. Wohn, Contour evolution, neighborhood deformation, and global image flow: Planar surfaces in motion, *Intern. J. Robot. Res.* 4: 95–108, 1985.
31. K. Wohn and A.M. Waxman, The analytic structure of image flows: Deformation and segmentation, *Comput. Vis. Graph. Image Process.* 49: 127–151, 1990.
32. K.Y. Wohn, J. Wu, and R.W. Brocket, A contour-based recovery of image flow: Iterative transformation method, *IEEE Trans. Patt. Anal. Mach. Intell.* 13: 746–760, 1991.
33. T. Yoshida, Automatic derivative derivation system (in Japanese), *Trans. Inform. Process. Soc. Japan* 30(7): 799–806, 1989.